Kinetic Diameter effect on hydrocarbon differential permeability in carbonate reservoirs

Annette Rafaela Sirgado Benchimol

Thesis to obtain a Master of Science Degree in

Petroleum Engineering

Thesis Supervisors:

Professor Gustavo André Paneiro

Professor Francisco Manuel da Silva Lemos

Examination Committee:

Chairperson: Professor Leonardo Azevedo Guerra Raposo Pereira

Supervisor: Professor Gustavo André Paneiro

Committee: Doctor Hugo Daniel da Silva Pinto

October 2021

Declaration

I declare that this thesis, is an original work of my own and that it fulfils with all requisites of the Code of Conduct and Good Practices of the University of Lisbon.

This page intentionally left in blank

Acknowledgments

The existence and development of this master thesis would not be possible without the support, assistance, and guidance of a group of people.

Firstly, my supervisors, Professor Gustavo André Paneiro and Professor Francisco Manuel da Silva Lemos who have always made time to supervise, help and pass through me all the scientific, theoretical, and technical knowledge that I required. I also want to express my gratitude to Professor Maria Amélia Lemos who also helped me throughout the chemical laboratory equipment and always gave her scientific perspective on the analysis of results.

My special thanks to Doctor Hugo Pinto for his research and who made himself available to clear my doubts and on the development of this work.

Many thanks to the staff of GEOLAB/LAMPIST for their contributions to the research and availability, namely Mr. Fernandes and Mr. Paulo. Also, I would like to thank my colleagues, Clive and Sérgio, for helping me to manoeuvre the laboratory equipment.

I would like to thank to my colleague and friend, Ana Sofia Marinho, who always listened to my concerns, encouraged me to study and not quitting not only through the thesis but throughout the hole master's course, especially during the pandemic. To my friends, Rita Lima and Isis Viana, thank you for the continued love, support, for making my days happier and for showing me the bright side of things.

Finally, I would like to thank to my sister, Kássia Benchimol, for always being with me through the bachelor and master, for the advice, encouragement and specially for the company on the lonely days far from my parents. To my mother, father, and brother, thank you for the opportunity of studying abroad, for always trying to provide me the best, for loving and supporting me, and for being a role model. Without you, none of this would have been possible.

Abstract

This thesis aims to understand the flow of reservoir fluids through a carbonate rock, relating to the fluid properties (porosity and permeability), and analyse the changes in composition of the mixture when crossing a porous media by using a versatile core flood system.

Also, a further study was performed in order to enhance knowledge about hydrocarbons homogeneous mixtures permeability when crossing carbonate samples. On that note, the core flood system was again applied for these oil mixtures analysis (isooctane / dodecane and isooctane / n-octane), to understand their overall behaviour and eventual changes in composition. The effluent collected from the injection of these oil mixtures was analysed, on the Gas Chromatograph equipment, to understand if it existed a preference flow of a particular component.

In addition, the results of this study were directly compared with the work of Doctor Hugo Pinto who performed similar analysis for a sandstone rock. With this comparison, it was possible to enhance the knowledge concerning the fluid flow of homogeneous oil mixtures in multiple porous media.

As a complement, analysis of seismic waves throughout a core sample was performed. The seismic waves analysis was conducted on dry and saturated core by using an ultrasonic equipment.

The work of this master thesis will provide a clearer insight in the fluid flow of reservoir rocks and will also serve as base for future research on this vast area.

Keywords: Carbonate rock / Porosity / Permeability / Core flooding / Kinetic diameter / Seismic waves / Hydrocarbons

Resumo

Esta tese visa compreender o escoamento de fluidos de reservatório através de uma rocha carbonatada, em relação às propriedades do fluido (porosidade e permeabilidade), e analisar as mudanças na composição da mistura ao atravessar um meio poroso, utilizando um sistema versátil de injeção de fluídos.

Além disso, um novo estudo foi realizado com o objetivo de aumentar o conhecimento sobre a permeabilidade de misturas homogêneas de hidrocarbonetos no escoamento em amostras carbonatadas. Nessa nota, o sistema de injeção de fluídos foi novamente aplicado para a análise dessas misturas de óleo (isooctano / dodecano e isooctano / n-octano), de forma a entender o seu comportamento geral e eventuais mudanças na sua composição. O efluente recolhido da injeção destas misturas de óleos foi analisado, com auxílio do equipamento Cromatógrafo a Gás, para verificar se existia um fluxo preferencial de um determinado componente.

Os resultados deste estudo foram comparados diretamente com o trabalho do Doutor Hugo Pinto que realizou análises semelhantes para um arenito. Com essa comparação, foi possível aumentar o conhecimento sobre o escoamento de misturas homogêneas de óleos em múltiplos meios porosos.

Como complemento, foi realizada a análise de ondas sísmicas ao longo de uma amostra de rocha. A análise das ondas sísmicas foi realizada com a amostra seca e saturada através de um equipamento ultrassônico.

O trabalho desta dissertação de mestrado fornecerá uma visão mais clara do fluxo de fluidos em rochas reservatório e também servirá de base para pesquisas futuras nesta vasta área.

Palavras-chave: Rocha Carbonatada / Porosidade / Permeabilidade / Injeção de fluídos / Diâmetro Cinético / Ondas sísmicas / hidrocarbonetos

Table of Contents

List of Figures

List of Tables

1. Introduction

Despite the growing of renewable energies, Crude oil and hydrocarbons in general are still the main traded commodity since these are some of the main fuel sources on our daily basis (Figure 1). As multiple crisis has emerged, namely in March 2020 when the oil price collapsed, it was noted an increase in the demand of cheap Arab Light oil by the USA and Urals oil by China to refill strategic reserves. This means that the activity in hydrocarbon energy sector has not receded. [1]

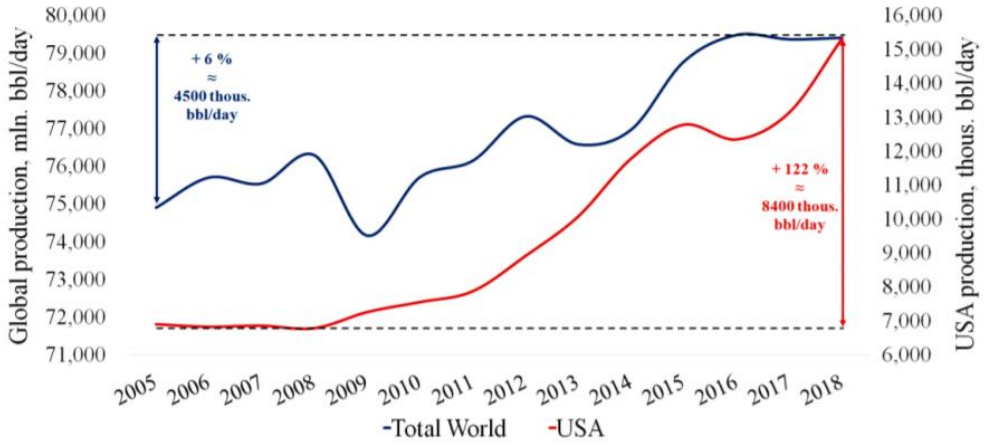

Figure 1 - Global and USA oil production dynamics. Based on BP Energy Overviews [1]

Given this, to answer the demand of oil production, the oil industry is still facing great technological development that leaded to the possibility to produce from reservoirs in severe conditions (e.g. severe temperature and pressure conditions), increasing possible reserves.

Typically, the first approach for oil extraction is Primary and Secondary oil Recovery. Primary oil Recovery is based on the natural rise (or via artificial lift systems) of hydrocarbons to the surface while Secondary oil Recovery depends on the injection of air and/or water which will provide a displacement of oil to the surface. [2]

With Tertiary Recovery or Enhanced oil Recovery (EOR) being a technique, which allows the extraction of up to 60% or more of the oil in the reservoir (depending on the employed EOR technique), compared to 20% to 30% if using just primary and secondary recovery, understanding its concept is vital. Enhanced oil Recovery seeks to alter oil properties, influencing as well rock-fluid interactions, as a means to make it more willing to extraction, this alteration can occur mechanically, chemically, thermally, and biologically. EOR has as main target to maximize the amount of oil recovered with the lowest possible cost from the existing fields before moving to the remote areas. [3]

With the purpose of improving hydrocarbons production, it is crucial to focus not only on the mechanisms that will allow the production, but also on their and the reservoir rock mainly properties from which hydrocarbons are going to be extracted, and the rock-fluid interaction. For instance, it was reported that a reduction in oil viscosity due to the high temperature fluid injection (hot water) accelerates the imbibition recovery rate. High temperature also impacts reservoir rock's wettability turning it more water-wet, which contributes to enhance oil recovery. [4]

Having that said, it is possible to conclude that a better understanding of rock properties and fluids characteristics can provide an improvement on EOR techniques.

1.1 Objectives

Core flooding, as a branch of EOR, is a laboratory test that replicates reservoir conditions with specific pressure, temperature, and flow rates. By injection, the fluids go through a rock sample filling up the pores and expelling the fluid that the rock was previously saturated with.

It is also important to take into consideration that oil is a very complex mixture of hydrocarbons and, although it is usually treated as a single fluid, even if it is a homogeneous mixture, flowing through a porous rock with very small pores, may induce changes in its composition. This also applies, in different ways, to many of the EOR techniques.

This thesis has as main purpose continuing the previous research of Chemical Transformations in EOR context, (Pinto, H. (2020). Universidade de Lisboa, Instituto Superior Técnico. Chemical Transformations in EOR context), specifically the effectiveness of coreflooding of binary oil mixtures isooctane / dodecane and isooctane / hexadecane in an oolitic carbonate rock.

On this previous work, several laboratory tests were performed in both oolitic carbonate and sandstone rocks such as determination of main properties (porosity and permeability), simulation of secondary and EOR recovery processes, core flooding of homogeneous binary oil mixtures, among others. However, no comparison between the two samples and influence of rock and fluid properties were made.

On this study, a carbonate rock, of the same origin as the thesis mentioned above, will be examined namely its main properties (porosity and permeability, p-waves velocity) which will be thoroughly estimated with the standard fluids (water, brine, and oil) present in EOR studies.

To complete this work, the flow of hydrocarbons molecules and hydrocarbons mixtures throughout the carbonate specimen and its characteristics at the end of the core flooding experiment will be analysed and compared with the results obtained for the sandstone rock. In addition, another hydrocarbon mixture will be added to this analysis namely, isooctane / n-octane, with the objective of studying the influence of the hydrocarbon structure on the mixture.

On this sequence, the effluents will be analysed on a Gas Chromatograph, which is an instrument that enables a sophisticated separation of blends, to show that homogeneous and binary mixtures have bulk

expulsion efficiencies, in other words, it will be used to draw conclusions on the way how oil mixtures cross reservoir rocks and if there is a natural preference for a component or if the flow is homogeneous.

Finally, the results of this study will be directly compared with the results obtained from the previous thesis developed over sandstones, and possibly a correlation will be made between the two rock specimens.

This work aims to understand whether rock and fluid properties have an influence in hydrocarbons fluid flow for different rock samples. Hopefully the results will provide more knowledge on this field of study and suggest further investigations.

1.2 Organization of the dissertation

This thesis is divided in five chapters being the first directed to the Introduction of this project where the motivation and objectives and organization of the dissertation are expressed.

The second chapter is focused on the Literature Review where the main properties and concepts, which are related and/or have an influence on the fluid flow, are described. In addition, it is also included a discussion of the previous works related to this field of study, mainly the research of Hugo Pinto, which served as a base for this thesis assumptions and conclusions.

After that, on the third chapter, it is described the Materials used on this research (rock sample, fluids, core flooding system, ultrasonic equipment, Gas chromatograph) as well as the Methods that were applied in order to obtain sample and fluid properties such as porosity and permeability of brine, and hydrocarbons individually and, finally, analyse hydrocarbons mixtures fluid flow so the influence of kinetic diameter could be studied.

On the fourth chapter are illustrated the Results based on the used methods, and it was also made an analysis based on the concepts and previous works mentioned along chapter two. Additionally, it was made a comparison between the results obtained from the carbonate sample and the sandstone rock from Hugo Pinto's thesis.

Finally, chapter five addresses the Conclusions of all of the work conducted, a more summarized analysis of the results and Future work suggestions that could possibly clarify some of the doubts raised on this thesis.

This page intentionally left in blank

2. Literature Review

2.1 Petroleum Production

Petroleum reservoirs go through several distinct phases throughout its life which will be referred here as a life cycle. This life cycle includes exploration, discovery, appraisal and delineation, development production, and abandonment. A brief introduction involved in the production of petroleum will be presented in this chapter. Production is also divided in multiple stages that are based on primary, secondary, and enhanced oil recovery (EOR) or tertiary processes. [2, 5, 6]

Primary recovery is associated with natural reservoir energy. This process of crude oil recovery is expressed by the initial crude oil production which often takes place by the expansion of fluids which were trapped under pressure in the reservoir rock. Once the initial pressure in the reservoir falls to a low value, the oil no longer flows to the wellbore, and pumps are installed to lift the crude oil to the surface, leading to the secondary recovery. When the initial energy has been depleted and the rate of oil recovery declines, oil production can be increased by the injection of secondary energy into the reservoir. [7]

After primary and secondary recovery, it is common for oil to remain in the reservoir and attempts to recover oil beyond primary and secondary recovery are referred to as tertiary recovery or enhanced recovery. Many of the EOR projects are implemented after waterflooding and include thermal, chemical, and miscible floods. These are employed by using an external source of energy to recover oil that cannot be produced economically by conventional primary and secondary means. [5, 7]

Table 1 - Production of conventional oil reservoirs [5]

Reservoir production	Typical recovery (%)	Notes
Primary	20–20	Production by natural drive mechanisms
Secondary	15–25	Mostly waterflood and gas injection
Tertiary	5–15	EOR methods

On Table 1, it is exposed the typical oil recovery percentage equivalent to each reservoir production mentioned.

2.1.1 Primary Recovery

Primary recovery, as mentioned before, is dependent on the natural energy of the reservoir, which is released gradually as the reservoir is produced. Oil recovery associated with natural reservoir energy varies with the producing mechanisms that are broadly classified as: solution-gas or depletion drive, gas cap drive, natural water drive, gravity drainage, compaction drive and liquid and rock expansion drive. If more than one mechanism is used, then it is referred as a combination drive. However, for most unconventional reservoirs, natural forces are inadequate to produce oil and gas thus, innovative techniques have to be applied. In the table below, it is found the circumstances where the primary production mechanisms can be applied. [2, 5, 7]

Table 2 - Primary drive mechanisms in oil reservoirs [5]

Reservoir type	Primary production mechanism	Estimated recovery	Gas–oil ratio at well	Water–oil ratio at well	Notes
Oil	Liquid and rock expansion	1–5%	None	Insignificant	Predominant mechanism when reservoir pressure is above the bubble point
Oil	Solution gas drive	10–30%	Increases to a maximum, then decreases	Insignificant	Predominant mechanism when reservoir pressure declines below the bubble point
Oil	Gas cap drive	30–40%	High in updip wells. Low in downdip wells	Insignificant	Energy provided by both solution gas and free gas in gas cap
Oil	Aquifer drive	Around 50%	Low	High in downdip wells	Water coning could be an issue for bottom water drive
Oil	Gravity segregation	50–80%	Low in downdip wells, and high in updip wells	Insignificant	Observed in fractured or high vertical permeability rocks. Typical recovery volume is low
Oil and gas	Rock compaction	10% or more	Depends on circumstance	Depends on circumstance	Production declines significantly following rock compaction

Summarizing, Table 2 shows primary production mechanisms in conventional oil and gas reservoirs and its variations on the recovery percentage for each mechanism. While the highest value corresponds to gravity segregation mechanism, the lowest corresponds to liquid and rock expansion.

2.1.2 Secondary Recovery

Secondary recovery is commonly applied when the pressure in the reservoir falls to a low value and primary recovery is no longer viable. However, the presence of a weak aquifer may lead to an early implementation of water injection to maintain reservoir pressure and improve oil recovery, in other words, it may lead directly to secondary mechanisms instead of primary [5, 7]. Conventional means of secondary recovery include the immiscible processes of waterflooding and gas injection. Secondary recovery can also operate as a pressure maintenance process which occurs simultaneously with primary recovery in order to prevent reservoir energy depletion. Pressure maintenance projects which can be

accomplished by the injection of either gas or water, will almost always recover more oil reserves than are recoverable by primary producing mechanisms. [2]

The preference between gas and water injection depends on reservoir composition for instance, in reservoirs with swelling clays or if permeability is very low gas injection are preferable since the rate of water injection may be very low. Water injection processes may be designed to: (1) dispose of brine water, (2) conduct a pressure maintenance project to maintain reservoir pressure when expansion of an aquifer or gas cap is insufficient to maintain pressure, or (3) implement a water drive or waterflood of oil after primary recovery. [7, 8]

Regarding to waterflooding (Figure 2), its goal is to augment ultimate recovery from the reservoir by injecting water to increase oil production and it has been the industry experience that generally 15−30% of OOIP (original oil in place) can be recovered. The basic concept is, inject water into the reservoir at high pressure to “push” or displace oil to the producing wells [5]. The effectiveness of waterflooding largely depends on rock and fluid characteristics, and how it is managed based on reservoir surveillance. For a waterflood project to be successful, some requirements are: homogeneous formations with favourable porosity and permeability (implies constant rock properties); absence of highly permeable conduits and fractures (to avoid channelling of displaced and displacing fluids); oil being light or medium gravity (20°API or greater); and relative high oil saturation. [5, 9, 10]

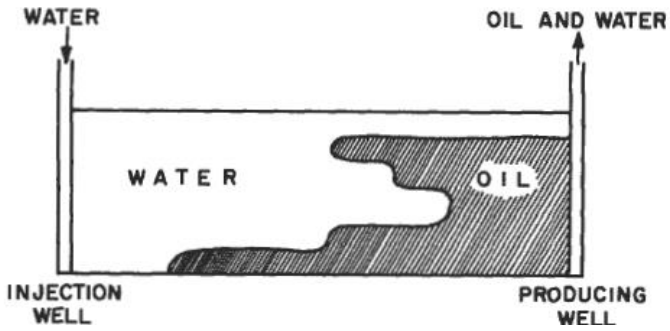

Figure 2 - Waterflooding schematics [5]

2.1.3 Tertiary Recovery / EOR Methods

The process of enhanced oil recovery has as ultimate goal the extraction of residual oil that could not and/or cannot be extracted by primary and secondary recovery processes. Worldwide statistic of petroleum reserves indicate that a vast portion of oil and gas remains on the reservoir due to the lack of available technology and unfavourable economics. Unrecovered oil in a conventional reservoir often exceeds half of the amount of petroleum initially in place (PIIP) [1, 2]. Having that said, EOR techniques are employed as a tertiary recovery process to recover the unexploited resources to the extent possible in a technological and economic sense. Certain EOR processes are not viable unless crude oil reaches a price point and can be broadly classified as: Thermal; Miscible; Immiscible; Chemical; and others.

However, due to high technical sensitivity of these methods and high cost of operation in reservoirs in the second half of their life, new EOR techniques are required. A general schematic of EOR process is depicted below. [11, 12]

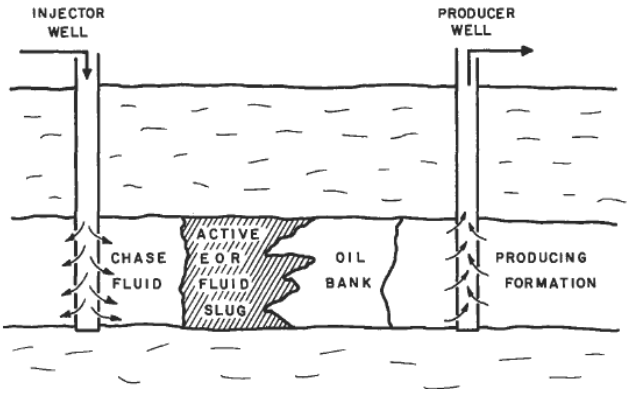

Figure 3 - General schematic of EOR [7]

Thermal EOR processes can be applied in conventional and unconventional reservoirs and are based on the reduction of the viscosity of crude oil by imparting heat (by steam or oil and combusted by air) to heavy oil therefore increasing its mobility in the reservoir. [4, 5]

Miscible processes are nonthermal and are applied in light to medium gravity oil. While thermal processes aimed to reduce oil viscosity, miscible processes reduce interfacial tension between fluids and significantly enhances the microscopic displacement processes. This is achieved when injected fluids mixes with *in situ oil* completely. On the other hand, immiscible processes are less efficient than miscible EOR and use as displacing fluid inert and flue gas. [5]

Chemical oil recovery methods include polymer, surfactant/polymer, and alkaline flooding, in other words, oil recovery is achieved by mixing chemicals in water prior to injection. Hence, chemical flooding is used for oils that are more viscous than those oils recovered by gas injection methods. [5, 13]

Other methods include microbial, acoustic, and electromagnetic which are still in an experimental stage with little documentation with exception of the microbial recovery that has been the subject of quite a number of studies. [12, 13]

EOR methods often require significant investment of capital and are generally associated with risks. No single method of EOR is effective for all reservoirs. EOR selection depends or the reservoir fluid and rock property, afterwards laboratory studies, reservoir simulation, and pilot flood are conducted before making an implementation. [5, 12, 13]

2.2 Reservoir rock and Fluid Properties

For conventional or fractured reservoirs, the understanding of rock and fluid properties is crucial because when combined with the geologic framework, log results and other statistics it provides a reasonable assessment of the reservoir performance. [14]

In order to obtain these properties, representative core samples or core plug samples, which is the case, are commonly obtained and exposed to laboratory examinations, core analysis. [15]

The core plug samples that will be used are not from the reservoir directly. Since it is not possible to obtain reservoir rocks (because of its constraints), outcrops are used as an alternative [16]. Outcrops of analogue reservoir rocks are potentially informative about the likely general attributes of fractures in the subsurface and are valuable because they provide distributed, two- and three-dimensional, rock data unaffected by borehole-based sampling limitations. In support of oilfield operations, a revolution is underway in rapid acquisition and processing of fracture observations from outcrop. [17]

An example of this situation is the oil field in the Sultanate of Oman, since it was not possible to obtain a representative core sample directly from the field because of the reservoir critical condition. Therefore, outcrop analogues were chosen as an alternative and its performance indicated the likelihood of significant internal heterogeneity and associated uncertainty. [16]

Beside rock and fluids individual characteristics, is as important to acknowledge rock-fluid interactions [18]. Therefore, detailed knowledge of reservoir rock and fluid properties is the backbone of almost all exploration and production-related activities.

2.2.1 Porosity

Although they are not visible macroscopically, natural fractures exist in all reservoir rocks, which will affect properties such as porosity. This, plus the grain diameters, will provide void spaces where petroleum reservoir fluids such as air, water, oil etc are going to be stored. Porosity is defined as a measure of these void spaces and describe the potential of reservoir fluids storage, hence the greater the amount of voids the rock contains, the greater the capacity to store petroleum reservoir fluids which imply a more porous reservoir rock material. Porosity, which is a static property, is one of several parameters required to characterize a porous material. [6, 14, 18]

Porosity, here denoted as Φ, is mathematically expressed as the ratio of the volume of the pores (PV) to the total bulk volume (BV) of the sample (usually expressed as a fraction or percent). [19]

$$\Phi = \frac{PV}{BV} \qquad \text{(Eq.1)}$$

Being the bulk volume the sum of the pore volume (void volume) and GV is the grain volume (volume of solid material):

$$\Phi = \frac{BV - GV}{BV} \quad \text{(Eq.2)}$$

One must distinguish between two types of porosities: total porosity and effective porosity, being total porosity the one mentioned on equations 1 and 2. As previously mentioned, all reservoir rocks have void spaces and not all of them are interconnected, which means it could reach a dead end, another void or closed pores (Figure 4). If they are interconnected, a network will be formed. Effective porosity, denoted as Φ_{eff}, is mathematically defined as the ratio of the volume of interconnected pores and the dead-end ones to the total or bulk volume of the sample. [6, 14, 18]

$$\Phi_{eff} = \frac{Vol.of\ interconnected\ pores + Vol\ of\ dead-end\ pores}{BV} \quad \text{(Eq.3)}$$

Effective porosity is of great significance from a reservoir engineering standpoint, since it represents the void space occupied by mobile recoverable hydrocarbon fluids. [18]

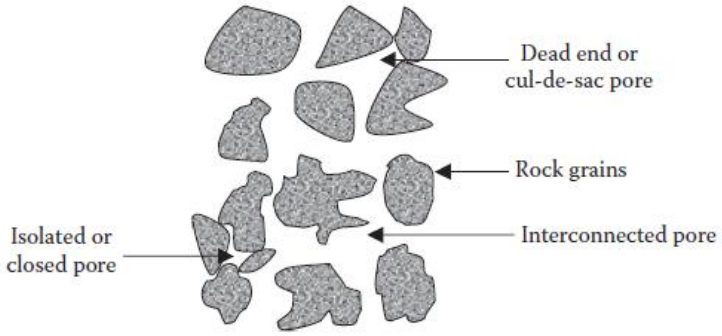

Figure 4 - Conceptual representation of different types of pores in a reservoir rock [18]

Porosity can also be classified by the mode of origin as primary or secondary. Primary porosity is defined as an original porosity, developed in the deposition of the sediments, while secondary porosity is related to an induced porosity developed during diagenesis and through production of fractures in the rock following the deposition of sediments. Rocks with primary porosity are more uniform in their characteristics than rocks with secondary porosity. [14, 18]

2.2.2 Measurement of Porosity

Determination of porosity of reservoir rocks can vary by two different methods: routine core analysis (laboratory measurements on core plugs drilled from whole core samples) and well logging techniques, being routine core analysis the most common one. These two methods differ on the conditions where the reservoir rock is found. While well logging techniques are indirect in nature and porosity is measured in situ, routine core analysis are direct, and samples are tested in laboratories. [18]

On this project, porosity measurements will be performed by routine core analysis.

As previously mentioned on Eq.1, porosity depends on pore, bulk, and grain volume. At least two independent measurements of the three volume contributors are needed to be determined (for dry and cleaned reservoir rock samples).

Regarding to cylindrical core plugs samples, the first step would be the determination of total bulk volume, BV, from the dimensions of the sample. It is important to understand that this method can lead to inaccuracies since it does not take in consideration the existence of irregularities resulting to unrepresentative BV and, subsequently, misleading porosities [18, 20, 21]. Archimedes principle is an alternative for this problem and states that the upward buoyant force that is exerted on a body immersed in a fluid, whether fully or partially, is proportional to the weight of the fluid that the body displaces. This principle has as an advantage the fact that it can estimate the BV of irregular shapes but, on the other hand, the fluid can penetrate the sample if the experiment takes too long which will also lead to an incorrect BV. To avoid this, the sample can be coated with paraffin wax, mercury or pre-saturated with the same fluid used for observing the displacement. Either way, if the sample is coated or pre-saturated, several measurements must be made to make corrections. [6, 20, 21].

Pore volume, PV, is related only to effective porosity since all methods related to these measurements imply a filling or extraction of fluid inside the pore spaces of the reservoir rock sample. So, these pores must be or interconnected pores or dead-end pores. For extraction of fluids, the common procedure is to subject the sample to solvents that will recover the total volume of the fluids contained in the pore spaces which will correspond automatically to the PV. On the other hand, for filling the sample with fluids, more methods, with 3 different varieties of fluids such as helium, water or synthetic oil, and mercury, can be applied [22, 23]. Following the same line of thoughts of the first case, the total volume of injected fluids will correspond to the PV related to the effective porosity since the fluid can only fill the interconnected and dead-end pores.

When introducing fluids into the pore spaced of the rock sample, helium is by far the most common method since it has clearer advantages over other gases and liquids: Helium is a clean inert and ideal gas (for pressures and temperatures employed in the process) and does not cause unwanted rock-fluid interactions that may alter the original porosity. In Helium porosimeters the principle of Boyle's law prevails, which is expressed by [21]:

$$PV = \text{constant} \qquad \text{(Eq.4)}$$

Where, P is pressure and V is volume.

The apparatus (Figure 5) of a helium porosimeter consist of two equal volume chambers namely reference and sample chamber. The reference chamber has a V_1 volume at initial pressure P_1 (usually 100 psig), and the sample chamber has an unknown volume V_2 with an equivalent pressure P_2 (atmospheric). By opening the valve to the sample chamber, the system reaches an equilibrium allowing then the determination of respective volume by the resultant equilibrium pressure P, Eq.5. [18].

$$P_1V_1 + P_2V_2 = P(V_1+V_2) \quad \text{(Eq.5)}$$

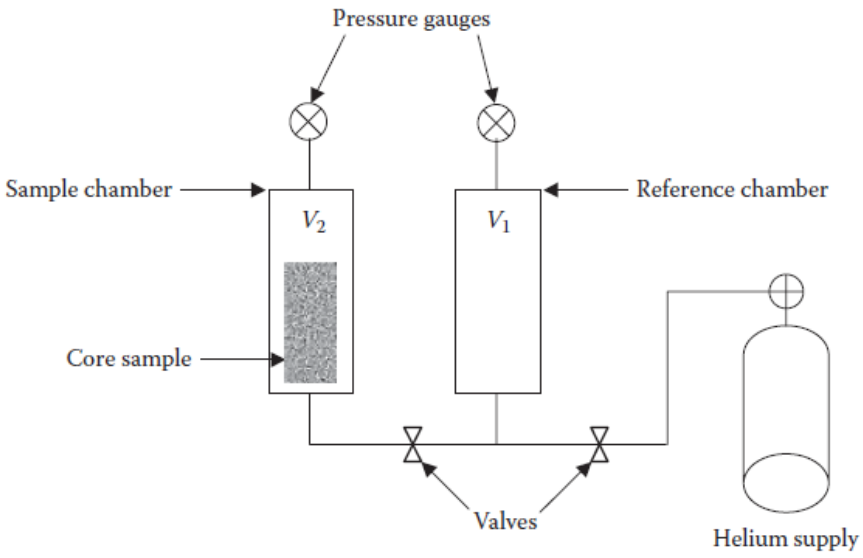

Figure 5 - Schematic illustration of a helium porosimeter [18]

Other liquid saturation methods into pore spaces of a reservoir rock sample involve forced saturation by either water or synthetic oil. This method is more complex and requires an advanced apparatus called core flooding rig. The sample is fixed in a core holder and liquids (water or oil) are injected through the sample by using a pump. [18, 20, 21]

Grain volume methods usually are related to total porosity or absolute porosity since the rocks are typically crushed to get grain volume which destroys all pore spaces. With that being said, grain volume results in total porosity as grain volume is subtracted from the bulk volume. Grain volume can also be calculated by dry samples weight and knowledge of average density. [18, 20, 21]

2.2.3 Permeability

The previous section addressed porosity or, basically the storage capacity of reservoir rock samples. Although having high porosity is necessary it is not a sufficient condition since petroleum fluids contained in these pores have to be able to flow so that they can be produced or brought to the surface from the reservoir. [18]

According to the Shclumberger's oil field glossary [24], permeability is expressed as the ability of a rock to transmit fluids, typically measured in darcies or millidarcies (m^2 in S.I. units). Permeability of a petroleum reservoir rock is one of the most influential parameters in determining the production capabilities of a hydrocarbon accumulation and is also a rock property depending on the pore space of rocks. It is also important to take in consideration that permeability is basically a flow property (dynamic) and therefore can be characterized only by conducting flow experiments in a reservoir rock. [6, 18]

In the year 1854 *Dupuit* made experiments with the urban filter in London. With a constant velocity, per day, he deduced that the pressure drop caused by the filter was proportional to the velocity of filtration. [19] Later in the year of 1856, in Dijon, *Henry Darcy,* a hydraulic engineer, proved this hypothesis and published the first definition of the fluid conductivity of a porous medium. [20] By developing a mathematical expression, still used today by the petroleum industry, Darcy expresses the calculation of permeability from flow experiments carried out in a porous media.

All his experiments were carried out by flowing water through tubes filled with sorted sand—from which he derived his final equation describing fluid flow. By considering a cylinder of porous media (Figure 6), Darcy's equation is only valid for the following assumptions: laminar (untrue for gases under certain flow rate conditions) and steady-state one-phase flow through a porous medium; the fluid should completely saturate the porous media; the fluid has to be largely incompressible; and the permeability is constant and does not vary with the nature of the fluid, flow rate nor pressure. [19]

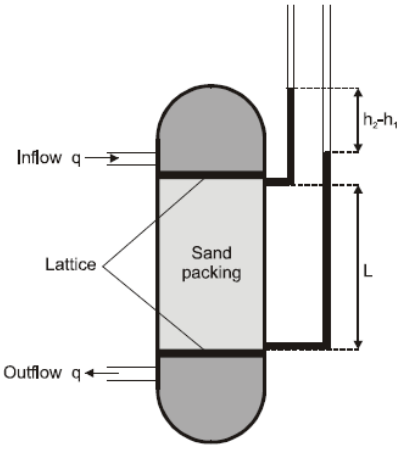

Figure 6 - Schematic diagram of Darcy's experiment [19]

$$Q = \frac{kA\,\Delta P}{\mu L} \qquad \text{(Eq.6)}$$

Where, Q[m³/s] is the fluid flow rate, $A[\mathrm{m}^2]$ is the cross-section of the porous medium perpendicular to the direction of the flow, k[m²] is the absolute permeability as a material property of the porous media, $\Delta P[\mathrm{N/m}^2]$ is the pressure difference along the porous medium, $\mu[\mathrm{N\ s/m}^2]$ is the viscosity of the flowing fluid, and $L[\mathrm{m}]$ is the length of the fluid pathway.

In addition, permeability can be classified in three principal kinds in core analysis: Absolute permeability, Effective permeability, and Relative permeability. [19, 25]

If a porous system is completely saturated with a single fluid, the permeability is a rock property and not a property of the flowing fluid (except for gases at low pressure). This permeability at 100% saturation of a single fluid is termed the absolute permeability [7]. Multi-phase flow is common in most petroleum reservoirs. In such multi-phase systems, we need to quantify the flow of each phase in the presence of other phases. [25] Effective permeability (k_o, k_w, k_g, for oil, water and gas, respectively), (Eq.7), is the permeability to one phase when two or three phases are present in the pore space while relative permeability (k_{ro}, k_{rw}, k_{rg}, , for oil, water and gas, respectively), (Eq.8), is the ratio of effective permeability of a particular fluid at a particular saturation to absolute permeability of that fluid at total saturation. Subsequently, relative permeability is a direct indicator of the ability of the porous medium to conduct a fluid when it shares the pore space with different phases. [20, 24]

$$\mathrm{qo} = \frac{koA\Delta Po}{\mu oL} \qquad \text{(Eq.7)}$$

$$\mathrm{kro} = \frac{ko}{k} \qquad \text{(Eq.8)}$$

And the same happens for k_w, k_g, k_{rw} and k_{rg}.

An example water-oil relative permeability plot vs. water saturation is given in Figure 7. Generally, the experiment is done in the direction of increasing water saturation to simulate water injection in the reservoir. There are two types of relative permeability curves: drainage curve and imbibition curve. On drainage curves, wetting phase saturation is decreasing which means the wetting phase is displaced by non-wetting phase. In contrast, on imbibition curves the wetting phase saturation is increasing meaning that non-wetting phase is displaced by wetting phase. As S_w increases, k_{ro} decreases and k_{rw} increases until reaching residual oil saturation. [6, 25]

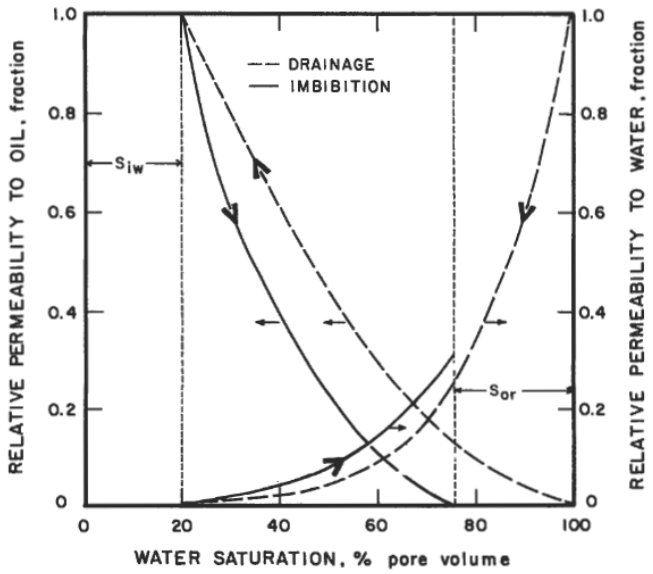

Figure 7 - Example of water-oil relative permeability data [7]

Several factors tend to affect relative permeability, for instance: Fluid saturations; Geometry of the pore spaces and pore size distribution; Wettability; and Fluid saturation history (i.e., imbibition or drainage). [7]

As seen in Figure 8, relative permeability to a particular fluid increases as the saturation of that fluid increases therefore fluid saturations have great influence on relative permeability. It was previously mentioned that permeability is related to porosity, thus a rock property depending on the pore space of rocks. Higher pore spaces imply higher permeability since permeability is a measure of the ability of a rock to transmit fluids through the pore network in the rock. Different rock characteristics are expected to produce different relative permeability curves. Regarding to wettability, in a strongly oil-wet system, water is expected to flow easier than in a strongly water-wet system. With that being said, it is possible to conclude that oil recovery, as a function of the water injected, is greater for water-wet cores than oil-wet cores. [7, 21, 25]

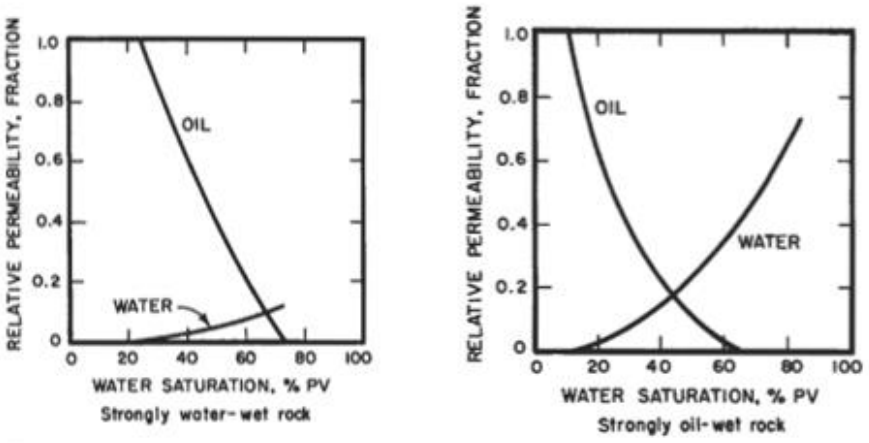

Figure 8 - strongly water-wet and strongly oil-wet relative permeability curves [7]

2.2.4 Measurement of Absolute Permeability

As stated before, absolute permeability is referred to the permeability when only one fluid is flowing. The most common method of measuring absolute permeability is the process of core-flooding a sample in the laboratory with a single-phase fluid until a steady state is obtained [5]. This measurement involves the direct application of the Darcy equation. The samples used are typically cylindrical core plug samples which are generally 1 or 1.5 in. in diameter with lengths varying from 2 to 4 in [18]. Samples from reservoir rocks must be thoroughly extracted from fluids and properly cleaned, dried, and placed in a vacuum chamber to expel all the air in pores prior the experiment [5, 20]. The method depends on the following factors: consolidation of the medium; core size; fluid properties; and the applied pressure.

The apparatus used for conducting flow experiments on core plug samples is a core flooding rig. The attainment of the steady-state fluid flow condition in the core sample is indicated by the same fluid flow rate at the inlet and outlet of the core, which corresponds to a constant pressure drop of the flowing fluid [5, 18].

Although core-flooding is the standard procedure for absolute permeability determination, a more robust approach is to record the differential pressure across the core for several flow rates and inlet pressures and a straight line is drawn through the experimental points. The slope of the line is a function of core permeability. [23]

The most common fluids used for the measurement of absolute permeability are formation waters, brine, or degassed crude oil. However, quite frequently these measurements are carried out using gases instead of liquids. Using gas as an alternative is simply convenient and practical since gas is clean, nonreactive and does not alter the pore network, hence, absolute permeability measurements are not influenced by any rock-fluid interactions. The experimental set up procedure for liquids is similar for gases (Figure 9). [5]

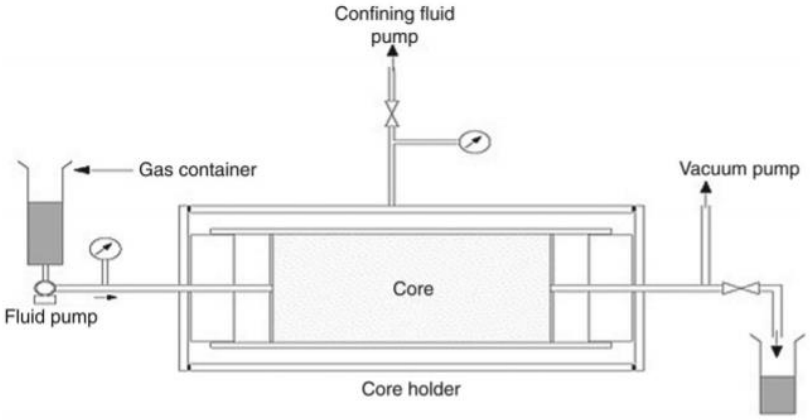

Figure 9 - Measurement of absolute permeability of a core sample using gas as injected fluid [5]

Darcy law was developed under the assumption of an incompressible fluid flow thus there is no accounting related to the compressibility of the fluids. The expected phenomena when an incompressible fluid flow takes place through a core sample of uniform cross section, the flow (Q/A) is constant at all sections along the flow path, however for gases this does not happen. For gases, since they are compressible, the pressure drops along the flow path results in a gas expansion which increases the flux thus, gas flux is not constant along the flow path, which implies modifications on the Darcy equation for calculation of permeability. [6, 18]

According to Klinkenberg in 1941, variations in the absolute permeability when using gases as the flowing fluid compared when using nonreactive liquids were noticed. When using gases, absolute permeability values are higher in comparison to liquids for the same core sample. This phenomenon is called gas slippage or Klinkenberg effect that occurs when the diameter of the capillary openings approaches the mean free path of the gas. [6, 18]

It is important to understand that the value of permeability obtained in the laboratory is likely to be affected by various factors, including the contrast between reservoir and laboratory environment, namely, pressure and temperature, integrity of rock during coring and core handling procedure from the field to the laboratory. [5]

2.2.5 Measurement of Relative Permeability

Relative Permeability can be obtained by two different laboratory methods: steady and unsteady state. Most of the literature considers that steady state techniques provide more accurate values that unsteady techniques. Yet, unsteady state techniques are much faster being less reliable and more economical to run. [26, 27]

For steady state, it is possible to apply Darcy's law to determine effective permeability for each phase at a given saturation. Two or three phases are injected simultaneously into the test core sample at constant rates and pressures (fixed gas-oil or water-oil ratio). Once steady state is reached, the outlet

flow rate of each phase and the pressure drop is measured and directly applied to the Darcy equation, which will give the effective permeability. [25] The process repeats itself until relative permeability curves for each phase are obtained. Steady state techniques are considered to be more reliable however, it can take an extremely long time for steady state to be reached at a given saturation level. There are numerous steady state methods available for instance, Penn State, Modified Penn State and Hassler methods, the Penn State being the most popular one. [6, 7, 27]

Unsteady state techniques are far more complicated. Fluids (either gas or water) are not injected simultaneously into the oil saturated core and saturation equilibrium is not achieved during the test. The test involves displacing in-situ fluids with a constant rate/pressure driving fluid. The outlet fluid composition and flow rate are measured and used in determining the relative permeability. Darcy's law is not applicable thus Buckley-Leverett equation for linear fluid displacement is the basis for all calculations. As previously mentioned, unsteady state techniques are less reliable since measurements are taken while the system is still changing over time however, they are the most common dynamic test. [6, 7, 25, 27]

2.2.6 Fluid saturation

From the last two chapters, it was stated the importance of porosity and permeability. Now, another characteristic related to porosity and permeability which is of great importance un reservoir engineering is fluid saturation. While porosity represents the amount of pore spaces present in a reservoir rock which will store reservoir fluid, fluid saturation or pore space saturation quantifies how much of this available capacity actually does contain various fluid phases; for instance, if referring to oil saturation (S_o) it is expressed as the ratio of pore space occupied by oil over the total pore space, the rest of the pore space is occupied by either gas or water or both (S_g, S_w). Therefore, the sum of the saturation of all fluid phases in fluid-fill pores would be 100%. [5, 18]

This knowledge is extremely important in the determination of initial hydrocarbon in place, inaccurate determination of initial fluid saturation often leads to expensive mistakes in the development of a field. [5, 6, 18]

The two main methods used to determine fluid saturations on core material (taken from the interval of interest) by extraction of the fluids are: The Retort method and the Dean-Stark extraction method. The retort method is also referred to as the summation of fluids porosity method while the Dean-Stark method is measured by heating and evaporating the fluids from the core and then condensing the vapours in a graduated tube. [5, 6, 20]

2.2.7 Mobility

Mobility of a fluid, λ, is essential for determining the characteristic of the displacement and it can be expressed as the ratio of effective permeability of the fluid to phase viscosity. [24]

Assuming a piston like displacement with the displaced fluid being oil and the displacing fluid being water, the Mobility ratio, M, would be the defined as the mobility, λw, of the displacing fluid, water, divided by the mobility, λo, of the displaced fluid, oil [28]:

$$Mow = \frac{\lambda w}{\lambda o} = \frac{kw \div \mu w}{ko \div \mu o} \quad \text{(Eq.9)}$$

When M $\leq$ 1, then the displaced fluid, oil, is more mobile than the displacing fluid which is beneficial for the displacement. However, when M $>$ 1, then the reverse situation is given, and it is considered an unfavourable displacement. (Figure 10)

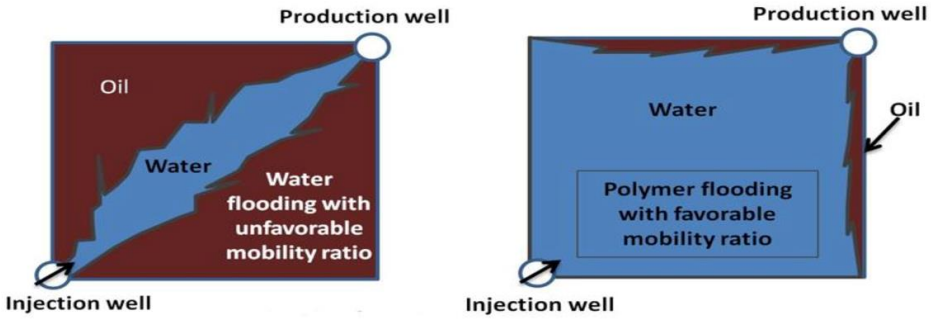

Figure 10 - Different displacements with unfavourable and favourable mobility ratio [29]

2.2.8 Wettability

Wettability plays an important role in the production of oil and gas as it not only determines the initial fluid distributions, but also is a major factor in the flow processes taking place within the reservoir rock. [3] Wettability of a reservoir-rock fluid system is the ability of one immiscible fluid in the presence of another to spread on the surface of the rock. The property of the rock is demonstrated by the fact that oil and water tend to spread and adhere to rock surfaces differently. [5, 19]

Wettability is identified by the contact angle, θ_c, of a droplet of a fluid with the surface area which it has spread out. Thus, the respective shape of the droplet depends on the wettability of the considered solid. In Figure 11, are presented two different cases of wettability, water-wet (a) and oil-wet (b). [5]

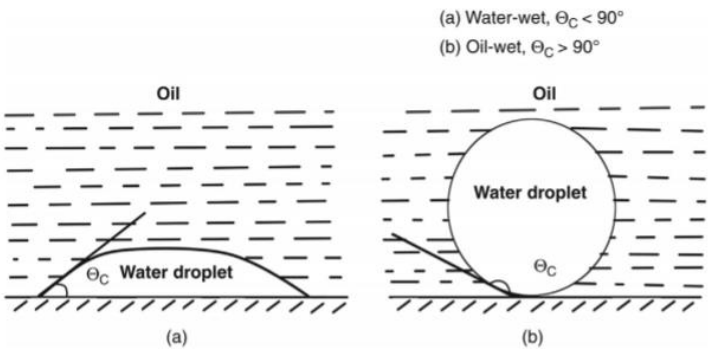

Figure 11 - Depiction of (a) water-wet and (b) oil-wet surface [5]

For water-wet rocks, droplets of water spread out to a greater surface area leading to a contact angle lower than 90°. In contrast, in oil wet rocks the droplets of water do not spread as much leading to a contact angle higher than 90°, then the fluid is considered as non-wetting. There are cases where the contact angle is about 90°, on this situation the reservoir exhibits intermediate or mixed wettability. [5]

Young, 150 years ago, defined the contact angle as a result of the static equilibrium, between a drop of liquid and a plane of a solid surface. The drop of fluid will take a certain shape due to the interfacial tensions acting on it, which are (Figure 12): the interfacial tension between fluid 1 and 2, σ_{121}; and the interfacial tensions between solid and fluids, σ_{s1} and σ_{s2}. [19]

Interfacial tension and the contact angle are temperature dependent.

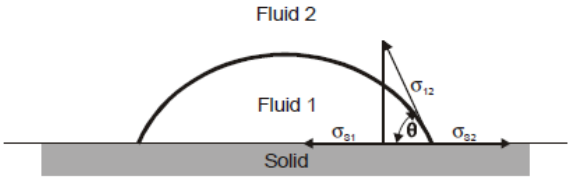

Figure 12 - Definition of the contact angle by Young [5]

.

The majority of oil reservoir rocks are known as water-wet, meaning that water will spread dominantly over oil in contact with the pore surface, although oil-wet reservoirs and intermediate wettability are not uncommon. [19]

Wettability of rock are the extremely importance regarding to oil recovery by waterflooding. In water-wet reservoirs, injected water displaces oil efficiently as oil has little tendency to adhere to the pore surface. [5]

2.2.9 Surface and Interfacial Tension

The term interface indicates a boundary or dividing line between two immiscible fluids. These interfaces can be liquid-gas, liquid-liquid, liquid-solid, solid-gas, and solid-solid, and are a few molecular diameters in thickness. Some of these interfaces are present in petroleum reservoirs since up to three fluid phases, gas, oil, and water may coexist although the attractive force between the molecules of oil is different than that of water or gas. [14, 18, 23]

When a liquid is in contact with air or the vapor of that liquid, the force per unit length required to create a unit surface area is usually referred as the surface tension (ST). [14] However, in the case of two immiscible liquids, the term interfacial tension (IFT) is used when describing the liquid-liquid interfacial forces. Regardless of being surface tensions or interfacial tensions, the physical forces that cause the boundary are the same. [18] Interfacial tension also affects other dynamic properties of rock, including wettability, capillary pressure, and relative permeability of rock to oil, gas, and water. [5]

Given the earlier definition of surface or interfacial tension, it has the dimensions of force per unit length usually expressed as mN/m or 10^{-3} N/m (dyn/cm) and commonly denoted by the Greek symbol σ. [18]

2.2.10 Capillary Pressure

When two immiscible fluid phases, such as oil and water, are present in a porous medium a pressure differential is observed between the two fluid phases that can be expressed as capillary pressure, P_c. Most important is the fact that capillary forces cause hydrocarbon entrapment since petroleum trapped in a reservoir represents an equilibrium state between gravity that wants to move the petroleum upward, which is resisted by capillary pressures. Capillary pressure is expressed as the difference between the pressure exerted by the nonwetting phase and the pressure exerted by the wetting phase. [5, 18]

$$\mathrm{Pc} = \mathrm{Pnw} - \mathrm{Pw} \qquad \text{(Eq.10)}$$

Capillary forces in petroleum reservoirs are a manifestation of the combination of IFT, wetting characteristics, and pore sizes of a given system. Based on early work in the nineteenth century of Laplace, Young and Plateau, a general expression for capillary pressure, P_c, as a function of interfacial tension, σ, and curvature of the interface is [14]:

$$Pc = \sigma\left(\frac{1}{r1} + \frac{1}{r2}\right) \qquad \text{(Eq.11)}$$

Where r1 and r2 are the principal radius of curvature at the interface.

In Figure 13, it is visible the effect of varying the wetting characteristics of the system and varying the radius of the capillary tube. On the right side, the wetting characteristics are the same, that is, the same IFT and contact angle, but the radius of the capillary tube is different compared to the left side. According

to (Eq.11), the capillary pressure is inversely proportional to the capillary tube radius, while the adhesion tension remains constant.

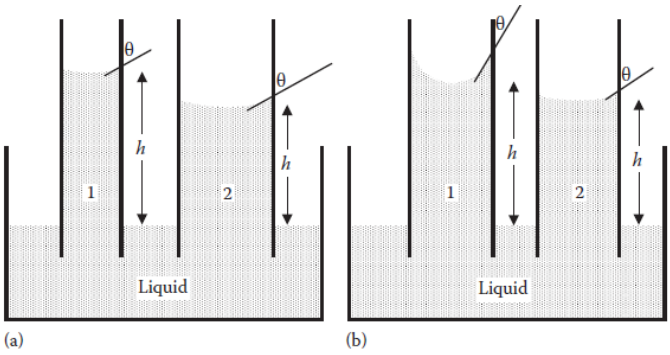

Figure 13 - Dependence of capillary pressure on wetting characteristics and pore size. (a) θ1 = θ, r1 ≠ r2; (b) θ1 = θ and r1=r2 [18]

Several methods to measure capillary pressure are the centrifuge method, porous diaphragm method, mercury injection method, and Leverett method.

2.2.11 Seismic Waves

In petroleum exploration, an accurate determination of potential areas to drill is fundamental. Information such as porosity, density and fluid content are essential, however these can only be obtained with certainty by drilling holes. Thus, a precise location for drilling must be selected and it can be obtained through seismic waves analysis which is by far the most widely non-destructive geophysical technique used for subsurface mapping. [30, 31]

Velocity and density contrasts between two layers, have always been a strong indicator of prospect areas since it causes a reflection of the seismic waves at the interface [32]. The study of seismic reservoir properties is an important aspect of reservoir characterization because with the use of seismic technology it is possible to directly link seismology to rock properties [31, 33]. Thus, a thorough understanding of seismic velocities in rocks plays a vital role in the success of the seismic methods.

Body waves can exist in two forms, compressional or primary (P waves) and shear waves or secondary (S waves). These are named body waves since they are the only ones that can travel through the inner layers of the Earth. Compressional body waves propagate by alternating compression and dilation in the direction of the waves. On the other hand, S waves have particle motion transverse to the direction of propagation (Figure 14). [30, 34, 35]

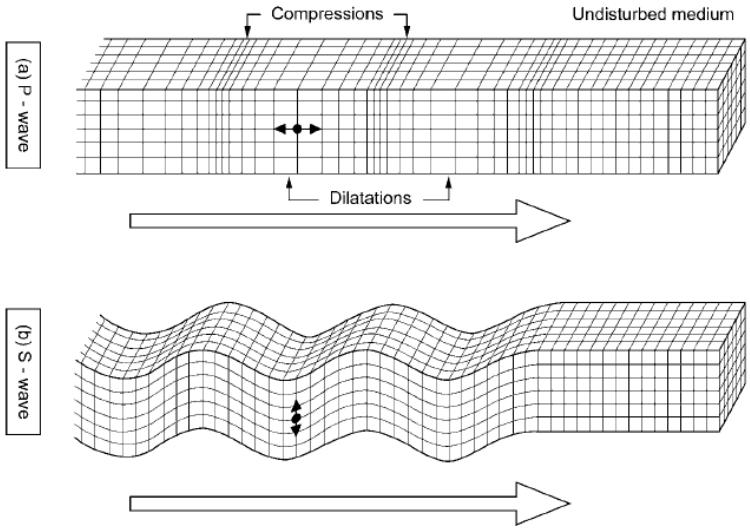

Figure 14 - Elastic deformations and particle motions associated with the propagation of body waves: a) P-wave, b) S-wave. [34]

These waves velocity is expressed in the following equations [33, 34]:

$$\mathrm{Vp} = \sqrt{\frac{\psi}{\gamma}} \quad \text{(Eq.12)}$$

$$\psi = \mathrm{K} + 4/3\mu \quad \text{(Eq.13)}$$

$$\mathrm{Vp} = \frac{\mathrm{K}+4/3\mu^{1/2}}{\gamma} \quad \text{(Eq.14)}$$

$$\mathrm{Vs} = \sqrt{\frac{\mu}{\gamma}} \quad \text{(Eq.15)}$$

Vp is the P-wave velocity (m/s), ψ is the axial modulus, K is Gassmann's bulk modulus, μ the shear modulus, γ is the density (kg/m^3) and Vs is the S-wave velocity (m/s).

Analysing the formulas, it is possible to notice that P-wave velocity is higher than S-wave velocity regardless of the scenario. Also, a media without any shear strength, despite the smaller Vp's, Vs is null. On this work only P-wave velocity will be analysed.

2.3 Differential Permeability effect in reservoir fluid flow

In this research, the most important aspect is to study the behaviour of hydrocarbons flowing throughout a reservoir rock, in this case, a carbonate rock. The origin and migration of petroleum is and has been a field of active discussion [36, 37].

Carbonate rocks are usually rich in the quantity of porous medium which makes them a good reservoir rock since natural fluids can easily percolate [36]. In addition, fluids not only percolate through rocks but also several interactions between the rock itself and the fluids occur during its flow [36]. It has been accepted for decades that systematic changes in petroleum composition occur during petroleum expulsion from the source rock (primary migration) followed by movement through carrier beds (secondary migration). [36, 37]

Chromatography is one of the main methods of chemical analysis and according to the official IUPAC and ASTM recommendations *a chromatographic system consists of two immiscible phases one of which is stationary and the other mobile (liquid, gas, supercritical fluid) and streaming over or past the stationary phase* (Jönsson 1987 [38]). Therefore, the existence of this method is dependent on the interaction of solute molecules of different types with the stationary phase and subsequently plays a role in the migration of subsurface fluids. [37-40]

One type of interaction is selective adsorption which is expressed under the condition that light and low-boiling hydrocarbons percolate first while higher boiling ones, flow later. Additionally, asphaltic matter and some high molecular hydrocarbons are removed from the liquid phase [38]. Mileshina *et al*. (1959) [41] described experiments in which crude oil was passed through quartz sand, clay minerals, feldspars, or calcite mixtures (Figure 15). In addition to chemical changes in the crude oil filtrates, selective adsorption of non-hydrocarbons constituents was also observed. [37]

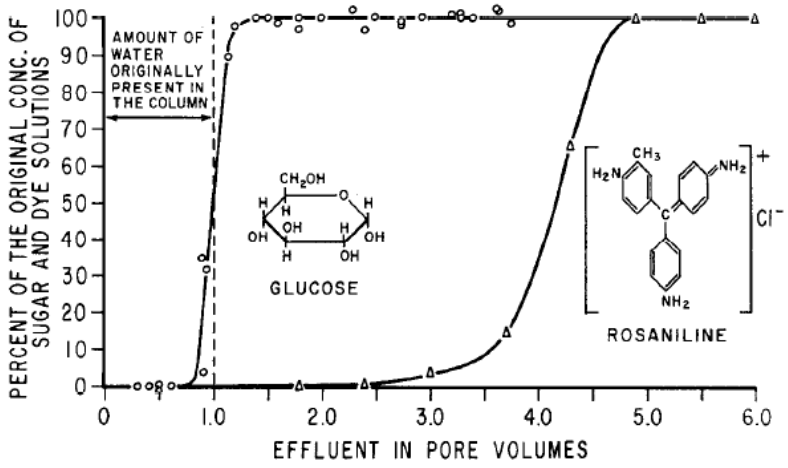

Figure 15 - Chromatographic effect in quartz sand columns [37]

To understand if the Chromatography process occurs, the solvent (glucose) will come out first and the solute (rosaniline) concentration will build up only after some pure solvent has accumulated in the effluent volume. If not, the effluent concentration will equal the concentration in the input fluid throughout the entire flow process [37]. Figure 15 shows that the concentration of rosaniline effluent did not increase appreciably until it reached the fourth mark in the Effluent in Pore Volumes axis. The effluent came out first and the flow of the solute was retarded in the column. This shows that chromatography was operational.

Chromatography is mainly seen in hydrocarbon generation and expulsion, for instance, cracking of kerogen to bitumen and the subsequent expulsion and migration (by a liquid or gas) of hydrocarbons into more porous and permeable carrier beds result in the formation of conventional petroleum deposits. The creation and expulsion of longer chain saturate products are more complicated because of the involvement of bitumen, in other words, the passage of crude oil through a solid porous may result in a retention of the high molecular weight and polar material. [37, 39]

It is theoretically reasonable to conclude that, during migration, certain constituents of a migrating oil may be selectively removed by solution in surrounding water and/or adsorption on rock surfaces. According to Leythaeuser et al. (1983) [42] for C_{15+} alkanes, the lower molecular weight components undergo migration more readily than higher molecular weight components and n-alkanes migrate faster than branched alkanes. Bonilla et al. (1986) [43] performed experiments which supported this theory.

Cheng and Huang [44] stated that there is a large adsorption selectivity of hydrocarbon gas molecules (C_1-C_6). Moreover, the results (Figure 16) reveal a strong preferential adsorption of wet hydrocarbon gases over methane, this conclusion confirms that the adsorption selectivity of hydrocarbon gases is closely related to their molecule weights, in other words, there is stronger adsorption for the heavier gas molecules. However, the applications of this study to the migration of hydrocarbon gases in the subsurface are limited.

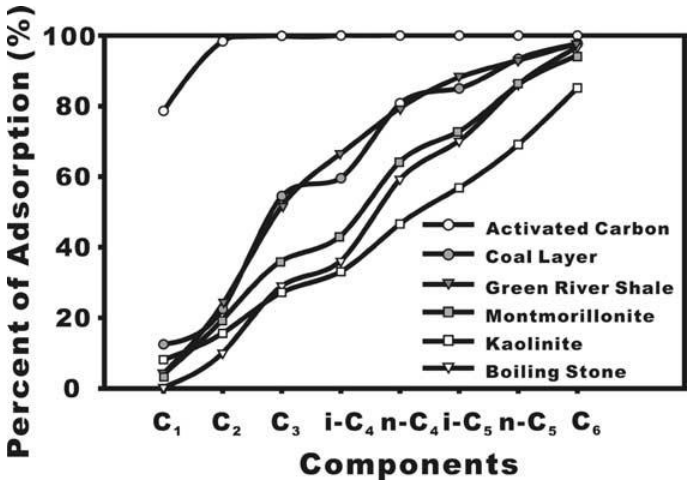

Figure 16 - Selective adsorption capacities of different hydrocarbon gases on the studied adsorbents near saturation measured at 1 atm total pressure and 26°C [44]

Migration of subsurface fluids can also involve no fracturing of the different phases, taking in consideration the movement of molecules from regions of high concentration to low concentration within a solution. This process is referred as diffusion or molecular transport and its role is highly dependent on the properties of the geological system and the transport mechanisms involved. It is also considered an important and efficient mechanism for the primary migration of light hydrocarbons. [45, 46]

The pioneering works of Antonov (1954, 1964, 1968,1970) [47-50] may be considered as the first attempts to study the diffusion of light hydrocarbons (C1-C8) in rocks of different lithologies. Most of these compounds are likely to be dissolved in the solid organic matter (kerogen) and the bitumen. From the kinetic theory of liquids (Eyring, 1936; Bradley, 1937; Wheeler, 1938) [51-53] a decrease of diffusion coefficients with increasing mass of the diffusing species is predicted following a $1/M^{-0,5}$ relationship where M is the molecular mass of the diffusing species. However, some studies report steeper decreases than expected for different lithologies with different conditions. [45, 46]

Kroos et al. (1988) [45] studies showed a decrease of diffusion coefficients with molecular mass for the C1-C5 hydrocarbons examined and, in most cases, can be described by a linear relationship.

2.4 Chemical transformations in EOR context

The study of hydrocarbons flow throughout a core sample was also analysed by Doctor Hugo Pinto [54] which, as mentioned multiple times, served as basis for this dissertation.

Pinto (2020) [54] studied the differential permeability in sandstone and carbonate rock samples. His work consisted of characterizing reservoir and fluid properties, physical and chemical mechanisms behind hydrocarbon recovery methods and a relation between these two concepts.

Furthermore, it was analysed how different classes of hydrocarbons homogeneous mixtures moved along these rocks considering different sample conditions and methods.

For the sandstone rock the sample was disaggregated, and the mixtures were isooctane / dodecane and isooctane / hexadecane in different mass proportions. The mixtures flow is expressed on Figure 17 to Figure 21 and the correspondent mass balances on Table 3 and Table 4.

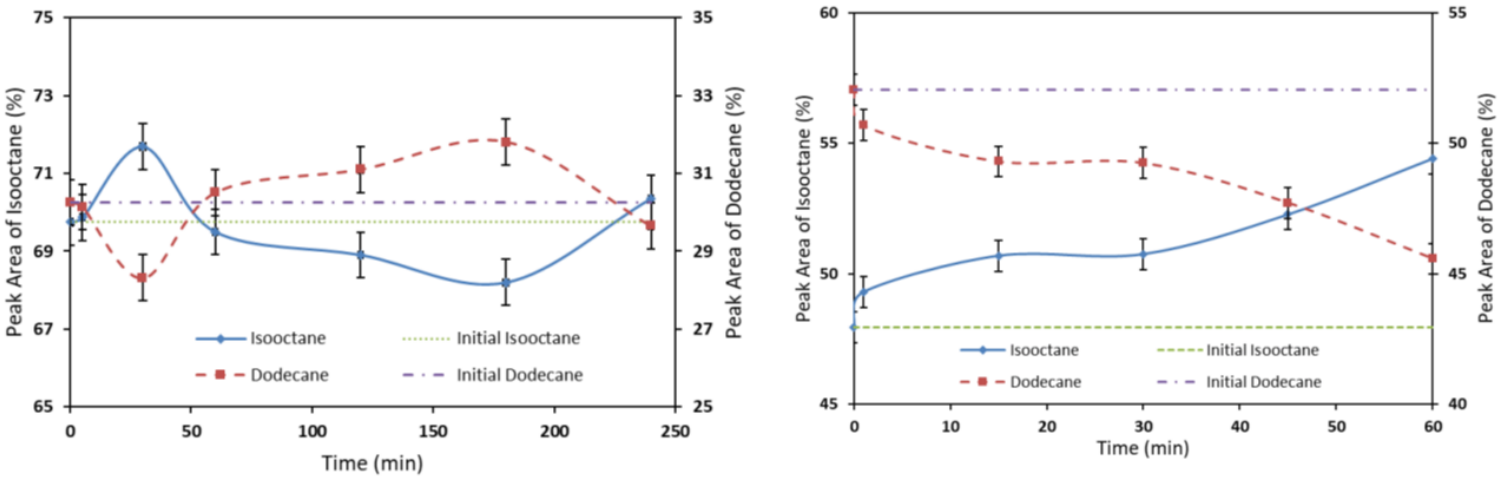

Figure 17 – a) Differential permeability for 69,7% Isooctane/ 30,3% Dodecane mixture; b) Differential permeability for 47,9% Isooctane / 52,1% Dodecane mixture [54]

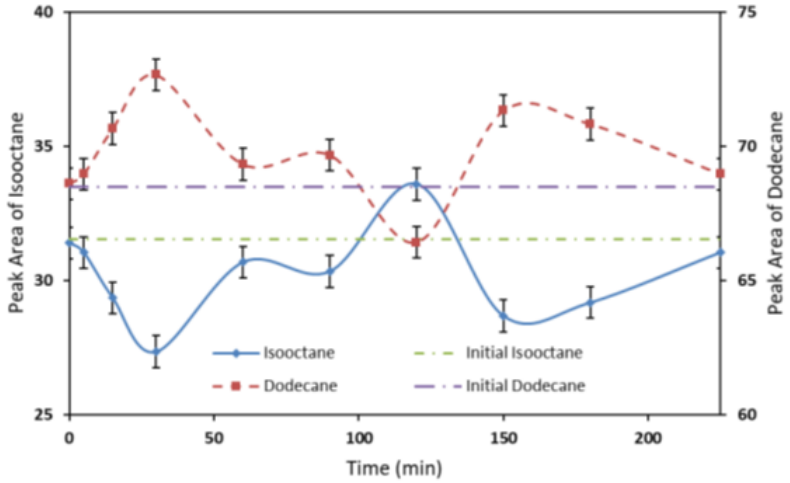

Figure 18 - Differential permeability for 31,5% Isooctane/ 68,5% Dodecane mixture [54]

Table 3 – Sandstone sample mass balance at isooctane / dodecane mixtures [54]

	Introduced Mass (%)		Collected Mass (%)	
	Isooctane	Dodecane	Isooctane	Dodecane
Mixtures	69.7	30.3	69.5	30.5
	47.9	52.1	50.8	49.2
	31.5	68.5	30.5	69.5

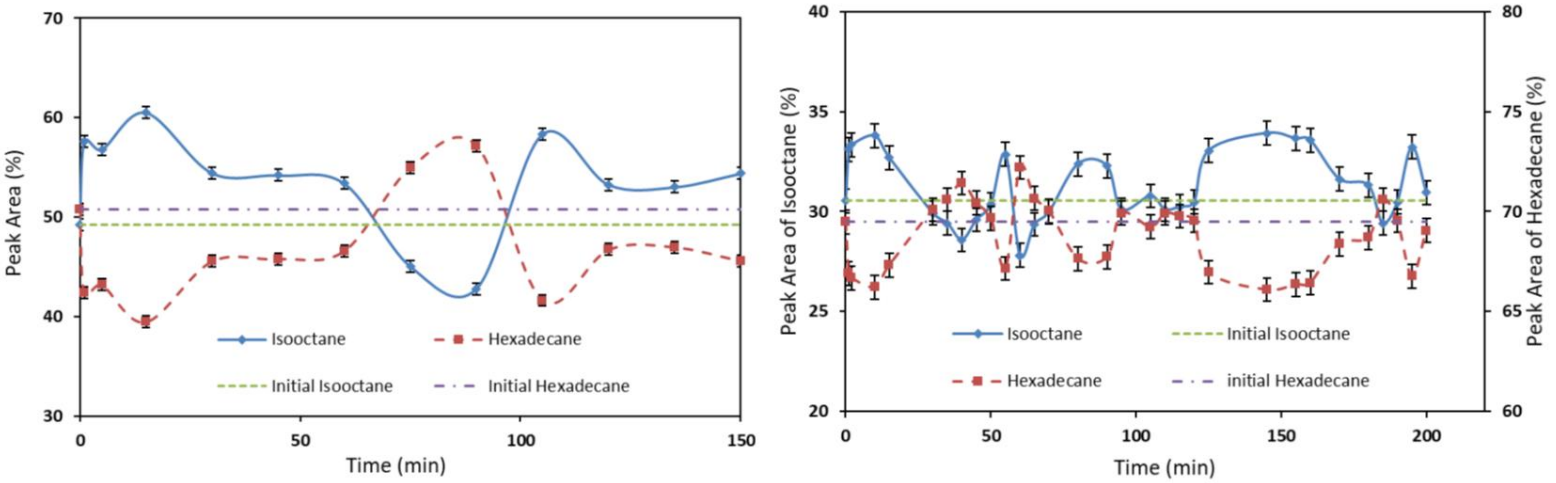

Figure 19 - a) Differential permeability for 49,2% Isooctane/ 50,8% Hexadecane mixture; b) Differential permeability for 30,5% Isooctane/ 69,5% Hexadecane mixture [54]

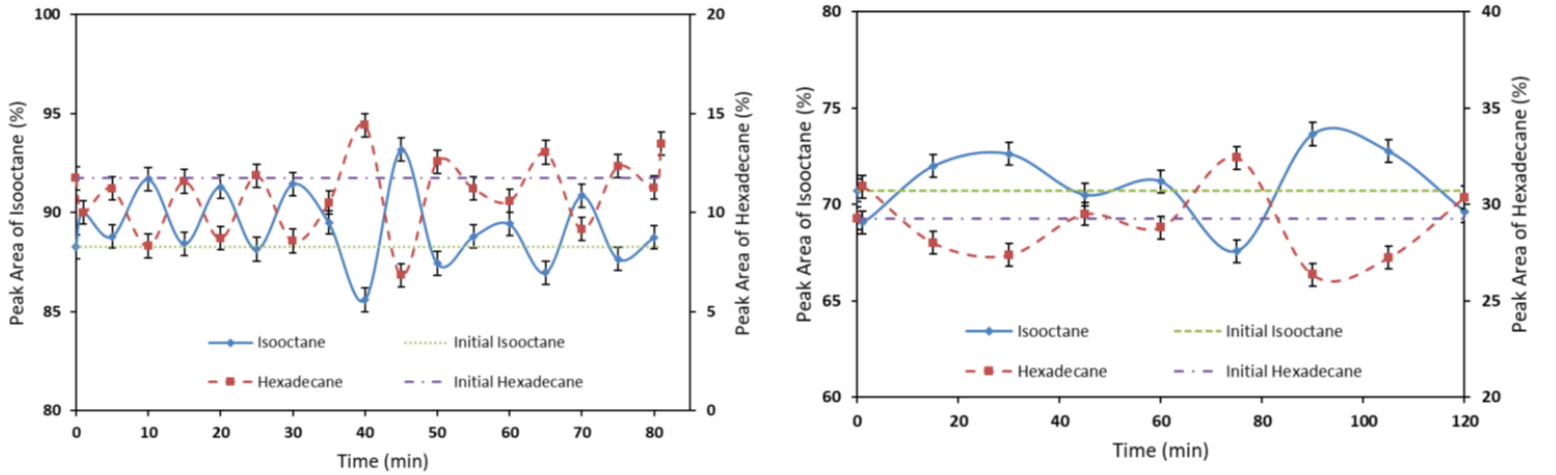

Figure 20 - a) Differential permeability for 88,3% Isooctane/ 11,7% Hexadecane mixture; b) Differential permeability for 70,7% Isooctane / 29,3% Hexadecane mixture [54]

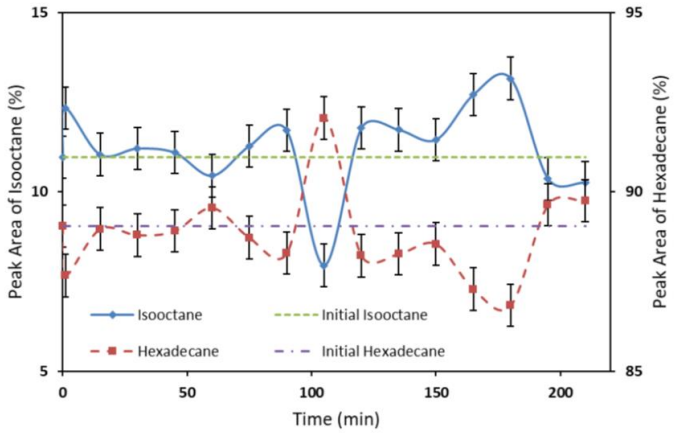

Figure 21 - Differential permeability for 11,0% Isooctane/ 89,0% Hexadecane mixture [54]

Table 4 -Sandstone sample mass balance at isooctane / hexadecane mixtures [54]

	Introduced Mass (%)		Collected Mass (%)	
	Isooctane	Hexadecane	Isooctane	Hexadecane
Mixtures	88.3	11.7	89.4	10.6
	70.7	29.3	71.2	28.8
	49.2	50.8	52.7	47.3
	30.5	69.5	31.6	68.4
	11.0	89.0	11.3	88.7

From Table 3, it can be noticed that for the first proportion, the collected and injected mass of the mixtures are similar. For the second, there is a higher amount of isooctane than dodecane at the collected mass and, for the third one, it was obtained a higher amount of dodecane at the collected mass. This oscillation is due to different assay time between these different mixtures and may be linked to the accumulation of the heavier species that results from the initial preferential flow of the lighter component.

Thus, as it can be seen in Table 4, there is a preferential flow of the lighter component, isooctane, during an initial period until hexadecane accumulations increases and subsequently its flow starts to increase.

These results are in accordance with the fact that higher molecular weight hydrocarbons have relatively higher dynamic viscosities, thus making them more difficult to flow, and primary petroleum migration favours light compounds, which was discussed in the previous chapter as well. [54]

For the carbonate rock the sample was consolidated, and the mixtures were isooctane / dodecane and isooctane / hexadecane in different mass proportions as well (Figure 22 to Figure 25, Table 5, Table 6).

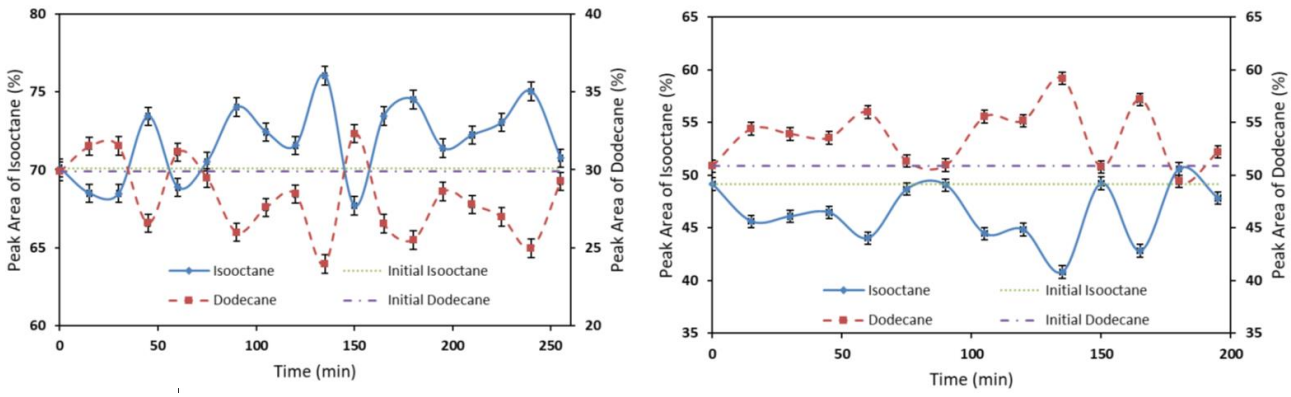

Figure 22 – a) Differential permeability for 70,1% Isooctane/ 29,9% Dodecane mixture; b) Differential permeability for 49,1% Isooctane/ 50,9% Dodecane mixture [54]

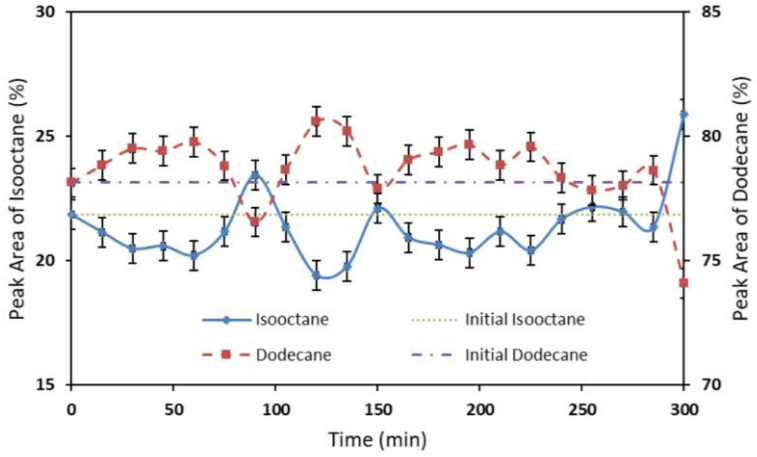

Figure 23 - Differential permeability for 21,9% Isooctane/ 78,1% Dodecane mixture [54]

Table 5 - Carbonate sample mass balance at isooctane / dodecane mixtures [54]

	Introduced Mass (%)		Collected Mass (%)	
	Isooctane	Dodecane	Isooctane	Dodecane
Mixtures	70.1	29.9	71.9	28.1
	49.1	50.9	46.0	54.0
	21.9	78.1	21.1	7.9

On the first essay it is noticed an accumulation of dodecane inside the core, which induces a preferential flow of isooctane therefore the collected mass of this component is higher. For the others two occurs an accumulation of isooctane enabling a preferential flow of dodecane.

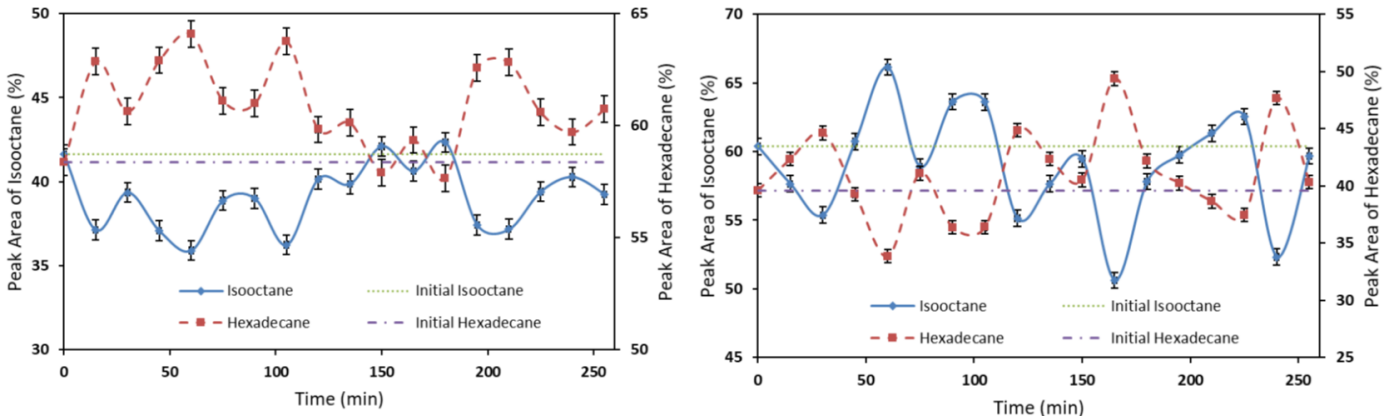

Figure 24- a) Differential permeability for 60,4% Isooctane/ 39,6% Hexadecane mixture; b) - Differential permeability for 41,6% Isooctane/ 58,4% Hexadecane mixture [54]

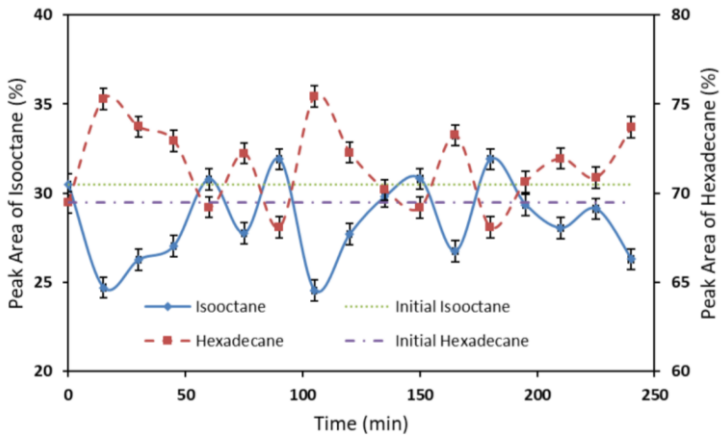

Figure 25 - Differential permeability for 30,5% Isooctane/ 69,5% Hexadecane mixture [54]

Table 6 - Carbonate sample mass balance at isooctane / hexadecane mixtures [54]

	Introduced Mass (%)		Collected Mass (%)	
	Isooctane	Hexadecane	Isooctane	Hexadecane
Mixtures	60.4	39.6	59.1	40.9
	41.6	58.4	38.9	61.1
	30.5	69.5	28.5	71.5

Analysing the introduced and collected mass percentages, the amount of hexadecane collected were always higher than the introduced for all the different proportions. Thus, an accumulation of isooctane inside the core occurs. Summarizing, for both hydrocarbons mixtures, a preferential flow of linear hydrocarbons happens, and it is more likely for the kinetic diameter to have an influence in this core sample then the sandstone since the rock was not only disaggregated but also presented larger pore sizes.

This page intentionally left in blank

3. Materials and Methods

In this chapter the background of the rock sample and fluids that were used is described, as well as the procedures implemented on this research to possibly correlate the main properties of the rock with the fluids, accomplishing then the main objective of the work.

It will also be described the apparatus of the core flooding system assembled for the experiments (and how it will be used to characterize rock properties), and the procedures performed on the carbonate sample, Chromatographic analysis. The workflow of this research is presented on Figure 26.

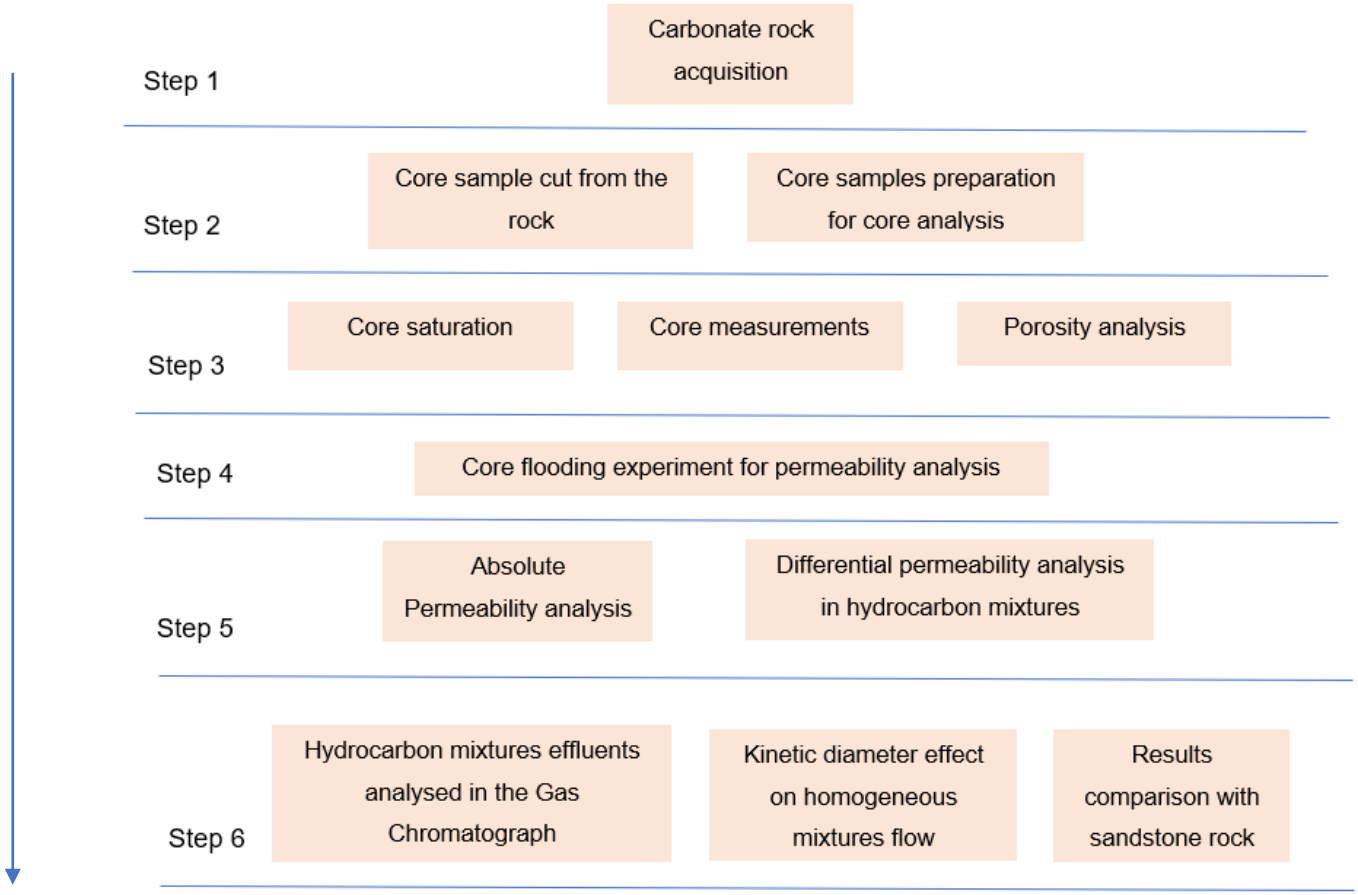

Figure 26 - Experimental part workflow

This process will be performed multiple times for different rock samples to guarantee representativeness of the results.

3.1 Materials

3.1.1 Carbonate rock

On this research the samples were obtained from Codaçal carbonate rocks. This choice took in consideration the fact that carbonate reservoirs represent the larger proportion of hydrocarbon reservoirs over the world, having its interest significantly regrown over the last decades [55, 56]. The specimens were collected in the surroundings of Alcanede and belongs to the Maciço Calcário Estremenho region. This area corresponds to a limestone massif that covers an area of 900 km^2 in the center of Portugal, around 150 km to the north of Lisbon. The productive units of the main ornamental varieties with origin in this thick carbonate sequence are dated of Middle Jurassic more specifically from the Bathonian period. [57-59]

Quarrying in Codaçal is restricted to a small place close to the township of the same name and is mapped in Figure 27 and Figure 28. These rocks are light cream coloured and fine to coarse granulometry oolitic bioclastic limestones with very thick beds, up to 16 meters, and are sub horizontal. [59]

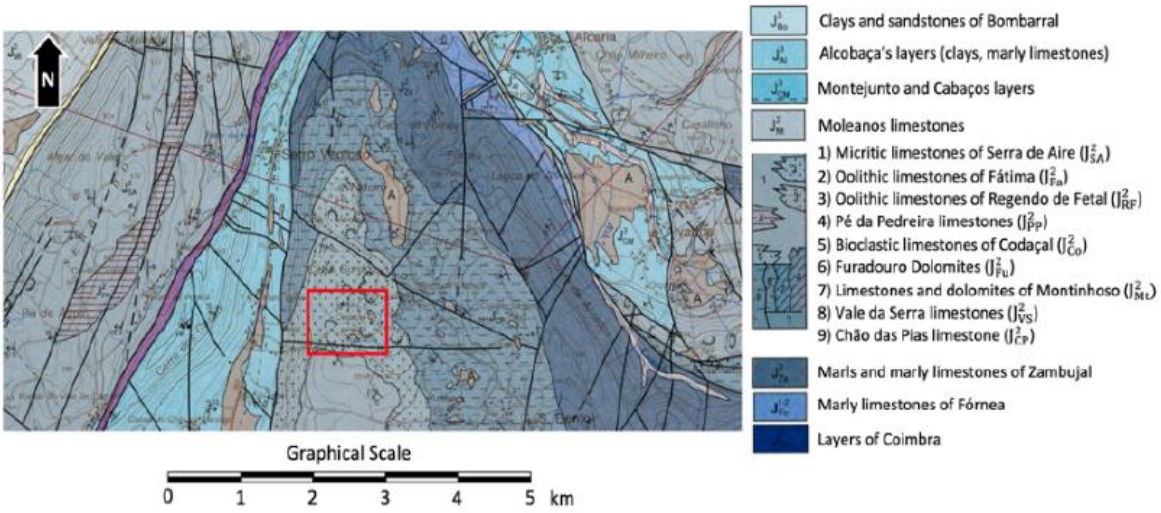

Figure 27 - Geological map of the studied area (adapted from Manupella et al. 2000) [60]

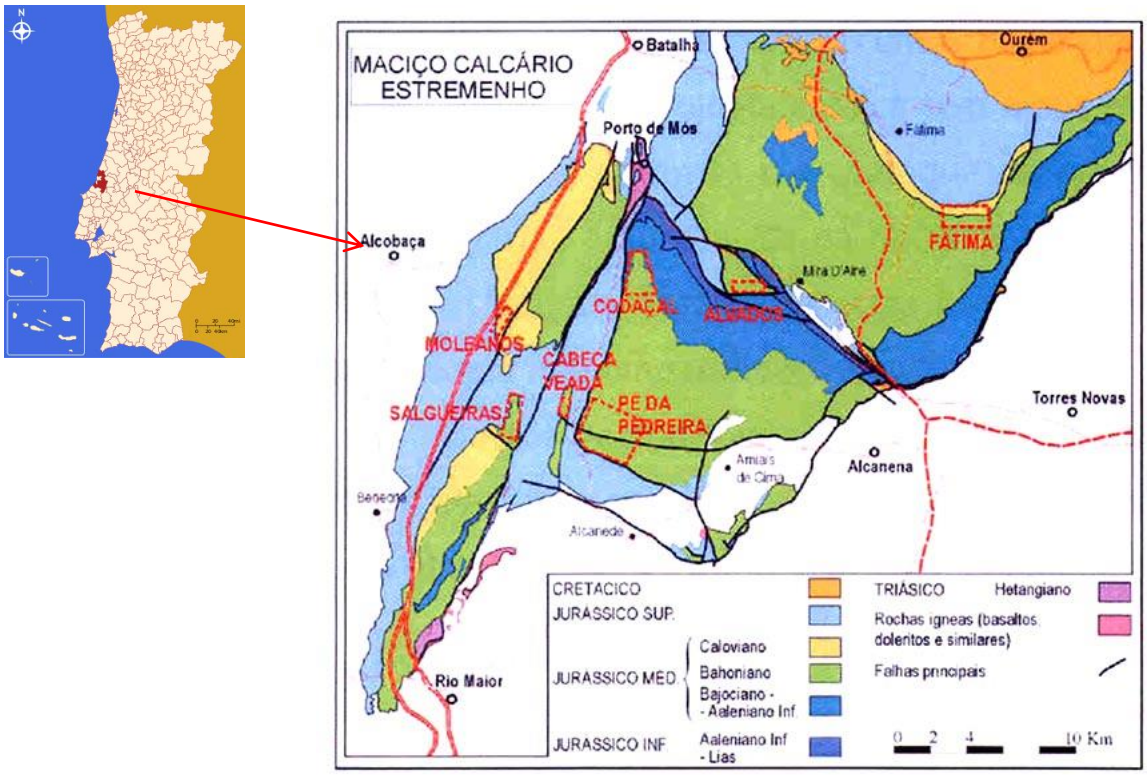

Figure 28 - Geological setting of the extractive centres in the Maciço Calcário Estremenho [59]

Portuguese limestones are mostly made of calcite carbonates ($CaCO_3$) and dolomite ($Ca,Mg\ CO_3$) [59]. In the following table it can be seen the mineralogical and chemical composition of the carbonate samples.

Table 7 - Mineralogical and Chemical composition of Codaçal carbonate samples [61]

Chemical Composition (%)	
CaO	55,86
Clay Minerals	43,6
Al_2O	0,54
MgO	0,1
K_2O	0,07
Si_2O	0,07
Na_2O	0,06

To obtain representative and reliable core analysis data, it is required to obtain high quality, undamaged core. Samples must be initially cleaned and dried to remove oil, water, and contaminants. Most routine core analysis tests are performed on plug samples cut from the full diameter core. The cores preparation

involved a specific mechanical machine (Figure 29a) which provided cylindrical forms with the tops cut in planes parallel to each other and perpendicular to the core axis. For consistency, all samples were taken in the same direction (either x or y) and discontinuities were avoided, nevertheless some geological variability is expected to be present on the analysed cores which will be around 38mm of diameter and length between 90 and 100 mm (Figure 29b). The rule of thumb is that the plugs for RCA (Routine Core Analysis) or SCAL (Special Core Analysis Laboratory) should have a length equivalent to one to two times the plug diameter. [20]

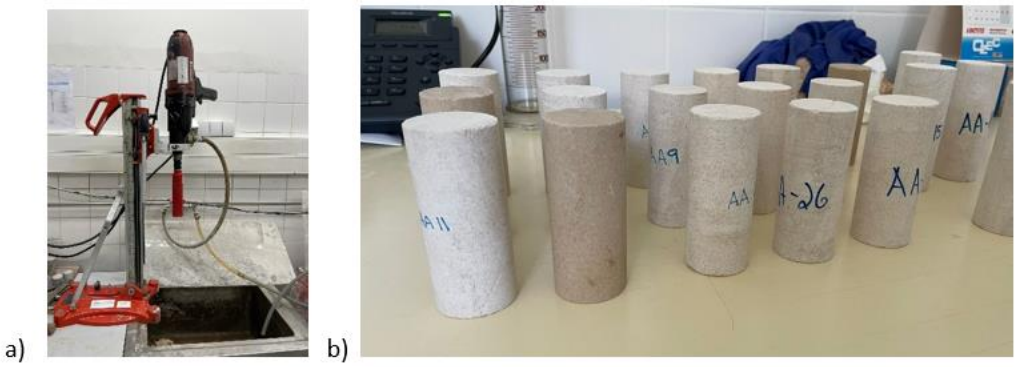

Figure 29 - a) Core drilling machine; b) Cores samples produced

For this thesis a total of twenty-five cores were cut on the same direction of the stratification, but not all of them were used.

To determine the samples bulk volume, the diameter (D) and length (L) were measured using a digital calliper with a resolution of 0,01mm and an average of the several measurements, for each core, was considered. Regarding to the mass of the core, a digital balance with resolution of 0,01g was used.

3.1.2 Fluids

The reservoir fluids used in this work were brine, distilled water, and four different synthetic oils. For brine, a sodium chloride solution was prepared dissolving 35 grams of NaCl by a litre of distilled water (0,6 mol/kg). Distilled water was also used, corresponding to a low salinity water. It´s properties are shown in the table below.

Table 8 - Water and Brine properties [62]

	Density at 25°C ρ (g.mL^{-1})	Dynamic viscosity at 25°C μ (cP)
Water	1	0,89
Brine	1,02	0,94

Regarding to the synthetic oils, to simulate reservoir oils, isooctane was selected as branched hydrocarbon, octane as the linear hydrocarbon with the same carbon number and hexadecane and dodecane as linear hydrocarbons with growing number of carbons. Octane / isooctane, dodecane / hexadecane have respectively 99,5% and higher than 99% purity.

Also, on this thesis different hydrocarbons mixtures were performed to analyse the influence of different kinetic diameters on the fluid flow throughout a core sample. Kinetic diameter is commonly referred as the space that a molecule occupies. [63]

The mixtures were isooctane / dodecane and isooctane / n-octane and its structure and properties, and of the remaining hydrocarbons used, are shown in Figure 30 and Table 9.

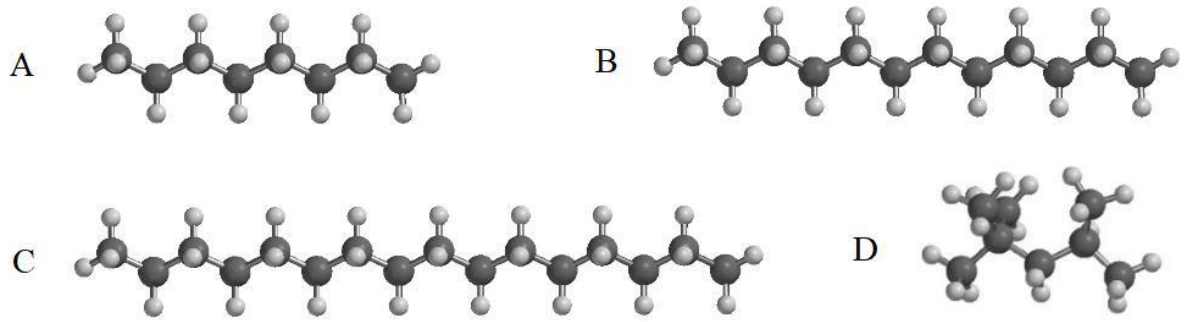

Figure 30 - Side view of n-octane (A), n-dodecane (B), n-hexadecane (C) and Isooctane (D). [54]

The synthetic oils isooctane and n-octane were obtained from the brand *PanReac AppliChem*, and dodecane and hexadecane from the brand *CamLab Chemicals*.

Table 9 - Hydrocarbon's properties [64]

Hydrocarbon	Molar Mass Mw ($g.mL^{-1}$)	Density at 25°C ρ ($g.mL^{-1}$)	Dynamic viscosity at 25°C μ (Pa.s)	Melting point (°C)	Boiling point (°C)
Isooctane	114,23	0,696	$5,10 \times 10^{-4}$	-107,38	99,24
Octane	114,23	0,703	$5,10 \times 10^{-4}$	-57	126
Dodecane	170,34	0,749	$1,30 \times 10^{-3}$	-9,3	218
Hexadecane	226,44	0,773	$3,40 \times 10^{-3}$	18,7	286,8

3.2 Core Flooding Tests

3.2.1 Core Flooding System Description

Core flooding procedures are commonly used in the petroleum industry, and it involves pressurized reservoir rocks to mimic reservoir conditions and flowing a fluid through it in the laboratory. The system used in this research is the same as the previous work [54] and was used to determine rock main properties.

The main components of the apparatus include a syringe pump, the core block, hydraulic hand pump, piston accumulators, a back-pressure regulator, and pressure transducers connected through a series of tubing and valves. Saturation and flooding agents of the core block are provided by the syringe pump and piston accumulators (Upstream). When the core block is saturated through its porous media, it is applied high pressures to simulate reservoir conditions. To simulate reservoir temperature, the core holder is inserted in a heating chamber and to maintain its temperature a thermal jacket is applied however this component was not used on this experiment. Finally, the fluid is collected from the core block and can contain from simple to two/three-phase separators if necessary (Downstream). [54, 65-67]

Core flooding tests can be performed at varying injection rates, temperatures, and pressure.

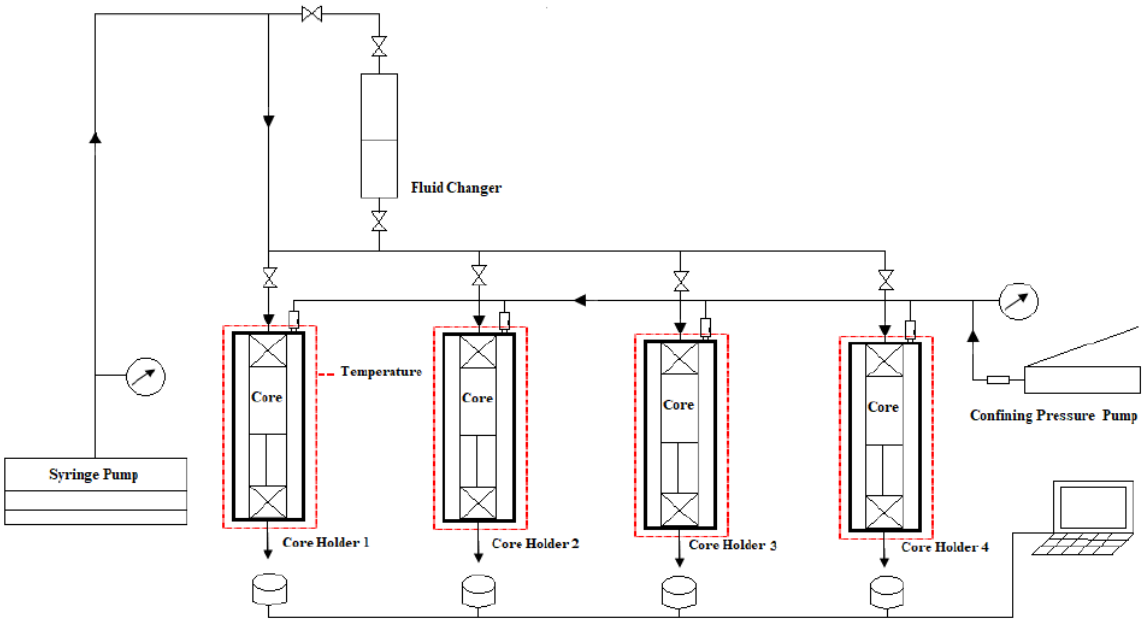

Figure 31 - Schematic core flooding experimental setup [59]

In the following figures are represented the syringe pump Pharmacia P-500 and the newest version of the same pump, with the same characteristics, that were used in this research. Both pumps provide an accurate and constant flow rate at pressure up to 5 MPa and are corrosive resistant. [67]

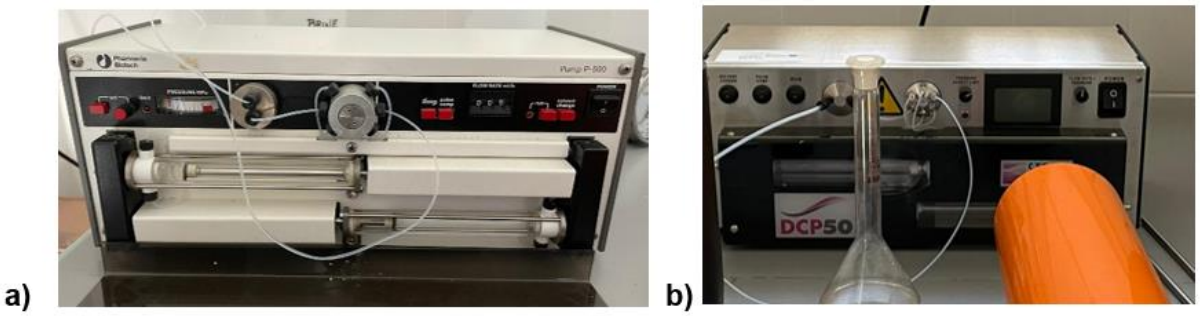

Figure 32 - Fluid injection syringe pumps: a) PharmaciaP-500; b) Strata Technologies DCP50

To increase measurements accuracy, a pressure gauge was added to outlet of the syringe pump. All the elements of the core flooding apparatus are connected by PEEK tubing system, which allows to work with a maximum pressure of 35 MPa without swelling or bursting and is corrosive resistant. This tubing does not interfere on the composition of the displacement fluids. It is also used a reducing union PEEK to connect syringe pumps and the core holders since the outside diameters of these elements are different. [67]

Regarding to the core block there are 4 core holders available made of stainless steel which can reach pressures and temperatures as well of 70 MPa and 150°C, respectively. The sample must have a diameter of 38mm and length up to 20cm due to the dimensions of the core holder. The sample is isolated from the confining pressure hydraulic fluid by a Viton sleeve. (Figure 33) [67]

Figure 33 - Core holder components and core plug sample

The confining pressure is applied to the core holder with a manual hydraulic pump ENERPAC model P 391 seen in Figure 34. On the right side of this figure, is visible a pressure gauge which function is to measure the confining pressure. This hydraulic pump has an oil tank capacity of 901 cm^3 and can reach a maximum pressure of 700 bar.

Figure 34 - Confining pressure system

All the material used in this apparatus including the ball valves and fitting products are made of stainless steel and can resist high pressures. Also, these materials are implemented in a way which increases the versatility of the system.

In the figure bellow is the overview of the core flooding experiment setup described.

Figure 35 - Core flooding setup

3.2.2 Porosity and Permeability Measurements

Core flooding systems are frequently used on characterization of reservoir rock properties. Effective porosity and permeability were measured for water and brine in different carbonate cores. These measurements will be made several times at different flow rates and confining pressures to guarantee the authenticity of the results. Porosity will be calculated according to Eq.2 and Eq.3 and permeability according to Darcy law (Eq.16).

$$K = \frac{Q\mu L}{A\Delta P} \quad \text{(Eq.16)}$$

Where K[m^2] is the permeability, Q[m^3/s] is the fluid flow rate, $\mu[\mathrm{N\ s/m^2}]$ is the viscosity of the flowing fluid, $L[\mathrm{m}]$ is the length of the fluid pathway, $A[\mathrm{m^2}]$ is the cross-section area and $\Delta P[\mathrm{N/m^2}]$ is the pressure difference.

3.2.3 Core saturation

According to the ISRM suggested methods, the core was saturated according to the following instructions. Firstly, it was dried in an oven at a temperature about 105°C for 24 hours. Secondly the diameter, length and dry weight of the sample as explained in chapter 1.1 was measured. Afterwards, the core was placed and vacuumed in an exicator (Figure 36) with the saturation fluid for approximately 2 hours in total. In the first hour the core was filled up until ¾ with the saturation fluid (distilled water) and vacuumed. After 1 hour the core was filled up until covering the surface with the fluid and vacuumed for an extra hour. Lastly, the core was kept inside the exicator (isolated) for another 24 hours.

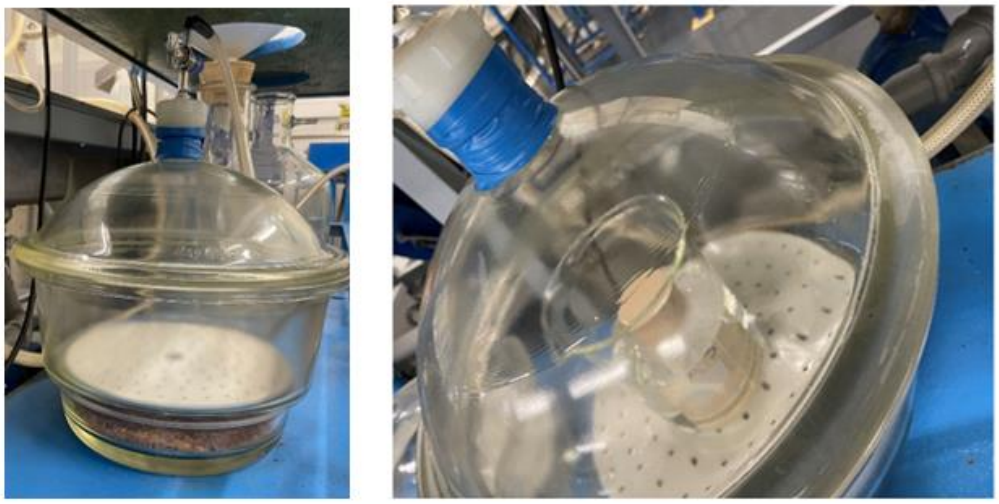

Figure 36 - Exicator used in the laboratory procedure with sample inside

3.2.4 Seismic Waves Propagation

The study of rock properties has been explained previously when porosity, fluid saturation and density was mentioned. Now, for seismic properties measuring, the method used was the pulse transmission (Birch, 1960). This method (Figure 37) assumes that ultrasonic seismic pulses are discharged by the pulse generator and converted to mechanical vibration by the transmitting piezoelectric transducer. After traveling through the rock sample, the elastic waves are converted back to an electrical signal by the receiving transducer. [32, 33]

The travel time of the acoustic waves can be measured on a digital oscilloscope so that the velocity values were calculated by dividing the length of core and the pulse transit time:

$$V_p = \frac{L}{\Delta t} \quad \text{(Eq.17)}$$

Where V_p is the P-waves velocity in m/s, L is the length of the core sample (m) and, Δt is the travel time (s).

Transducers were pressed to either end of the sample and the pulse transit time recorded. The tests were repeated at least twice, and the average value was taken as P-wave velocity value.

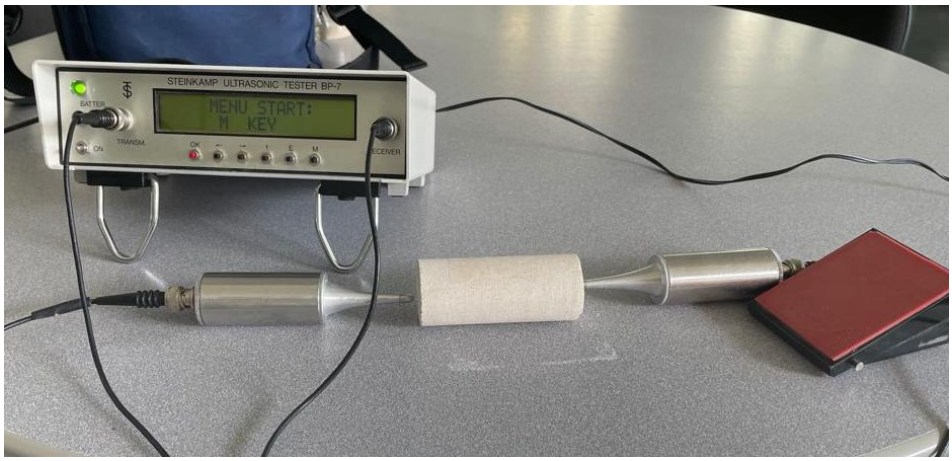

Figure 37 - Ultrasonic test equipment

Velocity measurements on the core sample were performed after the rock was dried and after saturation with different types of fluids: water, brine, and hydrocarbons. Also, rock properties as density and porosity were taken in consideration to analyse its influence in P-waves velocity variation.

3.2.5 Core Flooding

After saturation the core will be placed inside the Viton sleeve and inside de core holder. The core holder will be filled with the confining fluid (hydraulic fluid), without interfering with the core sample, and gradually the confinement pressure will be applied. The displacement fluid will percolate in the syringe pump and will be monitored at specific flow rate and injection pressure. Effluent weight will be measured during the procedure. As soon as the displacement fluid starts to flow in the outlet stream, the assay will be set for approximately 1 hour. Once the assay is done, the core will be removed from the core holder and weighted again. These assays will be performed at different confining pressures and flow rates for different analogous carbonate core samples for brine.

3.3 Differential Permeability Analysis and Gas Chromatography Analysis

The main objective of this study is to analyse how different synthetic fluids flow throughout the core samples and the interactions between the sample and the fluids for specific conditions of pressure and temperature. Previously, the apparatus of the core flooding process was explained and to complete the study, the collected fluid from the core samples will be examined. The fluids selected are simple binary oil mixtures isooctane/dodecane and isooctane/n-octane mixtures with varying proportions.

The cores were saturated with different isooctane/dodecane and isooctane/n-octane mixtures according to saturation procedure previously mentioned. After the saturation process the samples were weighted and inserted in the core holder at a confining pressure of 50 bar. The syringe pump contained the hydrocarbon mixtures, and the essay was conducted at a 6mL/h injection flow rate. During the essay it

was measured the injection pressure and amount of mixture recovered. The mixture effluent was collected into several polytopes every 5 minutes for approximately 2 hours. The carbonate samples were then removed from the core holder and conserved in a refrigerator.

In a very short time, gas chromatography (GC) has become the premier technique for separation and analysis of volatile compounds, especially petrochemicals. It can be used to analyse gases and liquids [55]. According to the International Union of Pure and Applied Chemistry (IUPAC), "*Chromatography is a physical method of separation in which the components to be separated are distributed between two phases, one of which is stationary (stationary phase) while the other (the mobile phase) moves in a definite direction. Elution chromatography is a procedure in which the mobile phase is continuously passed through or along the chromatographic bed and the sample is fed into the system as a finite slug*". Here, the mobile phase is gas.

After the effluent from the core flooding experiment was collected during a certain time interval, these samples were introduced into the gas chromatograph. A detector then monitors the composition of the gas stream as it emerges from the column carrying separated components, and the resulting signals provide the input for data acquisition. The analysis was carried-out on a Shimadzu GC-9A gas chromatograph equipped with a 50-meter capillary column PLOT (KCl/Al2Cl3) under temperature programming, and an FID detector. Also, a split ratio of 100:1 was used in a split/split less injector. The gas chromatograph was coupled to a Shimadzu C-R3A integrator. Again, this procedure follows the same premisses as previous research [54, 68]. The chromatograph then provides the mass percentages of each component that are contained in the injected sample. Appendix 1 summarizes the GC specifications applied on this study.

4. Results

Hydrocarbon reservoirs are porous and permeable rock bodies. In the broad sense, reservoir studies include reservoir geology, reservoir characterization, and reservoir engineering [70]. On this chapter is presented the reservoir rock sample characterization and exposed the results obtained throughout the experiment (porosity and permeability measurements, and reservoir fluid saturations).

4.1 Carbonate Porosity and Permeability Analysis

Porosity and permeability are important for rock characterization, for that different carbonate cores were tested for water and brine, respectively.

Since one of the objectives of this work is to compare values from the previous work of Pinto (2020) [54], it was important to assure that the cores had similar porosities and permeabilities so there is not a big variance in the final results. In other words, it was important to obtain the same initial results to guarantee a similar result, eliminating all possible errors associated to the process.

The initial carbonate cores samples collected didn't correspond to the ones expected since they presented different characteristics in terms of porosity and permeability values. Therefore, other rock samples had to be recollected so we could guarantee a precise work.

For porosity measurements only water was used. All the cores were measured for this property to make sure this new rock sample was reproducing the expected results.

For permeability, the tests were repeated for different injections flow rates (3 and 6 mL/h) and the same confining pressure of 50 bar. It was not possible to repeat the test for different confining pressures or for a higher flow rate in order to guarantee the rock integrity because the injection pressure was reaching values higher than the pressure gauge limit. On Table 10 are the characteristics of the analysed cores.

Table 10 - Characterization of cores in initial measurements and porosity

Core samples	Average Diameter (mm)	Average Length (mm)	Dry weight (g)	Porosity after water saturation (%)
1	37,82	90,57	241,51	10,35
2	37,88	90,57	243,99	9,75
3	37,93	90,47	235,05	12,92
4	37,87	90,62	234,08	13,52
5	37,93	90,39	241,16	10,38
6	37,90	90,47	234,88	13,19
7	37,88	90,31	242,67	10,15
8	37,85	90,47	240,46	10,78
9	37,90	90,53	244,69	9,34
10	37,92	90,50	242,36	10,38
11	37,91	90,66	244,54	9,61
12	37,87	90,29	235,07	12,62
13	37,90	90,62	242,03	10,59
14	37,89	90,67	241,59	10,76
15	37,94	100,22	265,51	11,69
16	37,75	101,34	271,17	10,42
17	37,73	101,05	274,41	9,75
18	37,70	100,85	263,67	12,31
19	37,85	99,96	271,16	9,27
20	37,87	100,86	268,25	11,61
21	37,83	91,70	237,88	12,56
22	37,88	91,61	244,37	10,75
23	37,89	91,50	245,52	10,18
24	37,84	91,21	245,27	9,70
25	37,92	91,57	246,73	9,54
26	37,87	91,61	247,02	9,65

Overall, the cores analysed presented porosities ranging from 9,27% to 13,52%, which correspond to the common ultimate porosity in carbonate rocks, 5-15% [70]. Again, the cores porosity was measured with water only. After these measurements, all samples were re-dried so they could be reused for further analysis.

It is possible to notice that there is a high variation on porosity values. It is true that higher values of porosity were expected since more than half of the samples presented porosities lower than 10%. According to Figueiredo et al. [71] and Alves et al. [72], an evaluation of the pore structure of Codaçal carbonates showed an open porosity value in the range of 11,2 and 12,8%. A low porosity may be associated to less pores, fractured pores caused by compression, among other reasons. However, it was not possible to evaluate the pore structure to analyse porosity values.

Regarding to the permeability, it was measured for different cores with different ranges of porosity to establish a connection between porosity and permeability. With that being said core1 with porosity of 10,35% and 4 of 13,52% were tested. The cores were saturated with brine and inserted on the core holder. The tests were performed for different flow rates and constant confining pressure (Table 11).

Table 11 - Brine permeability for different cores at different conditions

Core Samples	Porosity %	Permeability (mD) with Flow rate - 3 mL/h	Permeability (mD) with Flow rate - 6 mL/h
1	10,35	0,022	0,069
4	13,52	0,128	0,116

Permeability varies greatly in carbonate reservoirs from values of less than 0,1 mD in tight, crystalline mosaics in mudstones to over 10 Darcies in fracture, cavern, or connected vug systems [70].

When increasing the flow rate, it is possible to see a slight alteration on the permeability values however, it does not seem to have a relevant influence and it shouldn't because it is considered a Darcy flow. It is possible for this increase to be related to a higher availability of the porous media or interconnected pores, due to an increase of the injection pressure, supplying a higher flooding of the fluid.

Analysing the previous results, it is possible to observe that for sample 1, with lower porosity, correspond to a lower permeability for different flow rates when comparing to sample 4 with higher porosity. Therefore, it is possible that exists a correlation between porosity and permeability values, higher the porosity may imply a higher permeability. Having this possibility in mind, on further tests, the samples of higher porosity were prioritized to achieve higher permeability values, which was the ideal.

As mentioned before, the tests were conducted for a constant confining pressure to preserve rock integrity. When higher confining pressures were applied, the injection pressure passed the gauge limit

and when this didn't happen, the permeability values were lower than expected. According to Ghabezloo et al. [73], permeability decreases with the confining pressure increase for a constant average pore pressure (Figure 38). Thus, under a constant confining pressure, the permeability increases with the pore pressure increase, which was the scenario implemented on the core flooding test.

In summary, the effect of the pore pressure change on the variation of the permeability is more important that the effect of a change in the confining pressure.

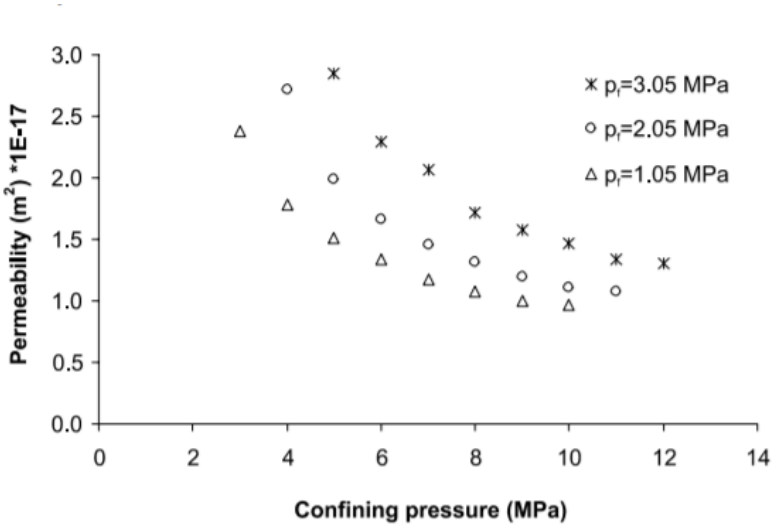

Figure 38 - Measured permeability as a function of the confining pressure for different average pore pressures [73]

4.2 Seismic Waves Propagation

With different conditions of pressure, temperature, and flooding agents, rocks samples present different values of velocity [32]. It is interesting to understand how carbonate rock samples behave when saturated with different flooding agents. An accurate knowledge of core behaviour can possibly indicate hydrocarbon presence on rock samples. It is also important to take in consideration that rocks have unconformities, different pore sizes, and faults that could have an influence in velocity results. [30, 34, 74]

Gregory et al. [31, 75], studied the influence of saturation by water, oil, gas, and mixtures of these fluids on the densities, velocities, and other characteristics of consolidated sedimentary rocks in the laboratory by ultrasonic wave propagation methods. With this study was concluded that fluid saturation effects on compressional wave velocity are much significant in low-porosity than in high-porosity rocks [76]. In addition, Lama and Vutukuri [77] showed that the wetting of rocks usually indicates a rise in the P-wave velocities.

From Table 29 and Table 30 present on Appendix 2 are the sample measurements and velocity results after drying and saturating the rock samples with water. With these values the following graphs (Figure 39 and Figure 40) representing the relation between P-waves velocity and density and P-waves velocity and porosity (with different saturation fluids) were made.

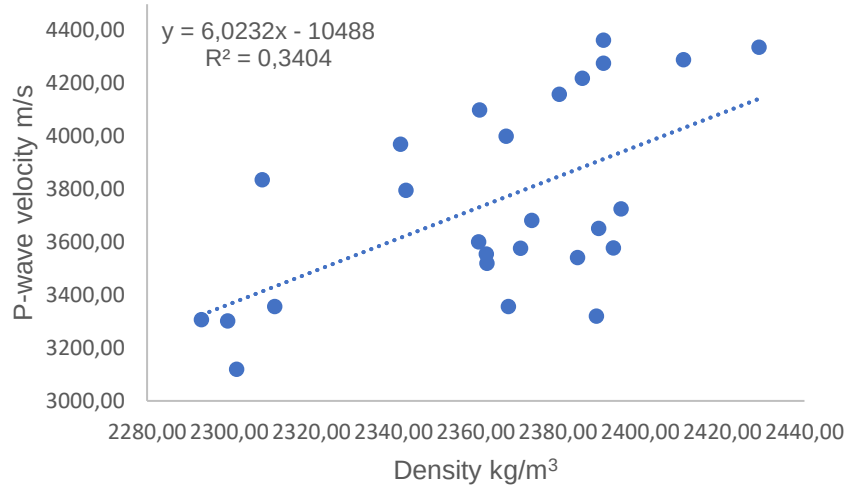

Figure 39 - P-wave velocity Vs carbonate rock density

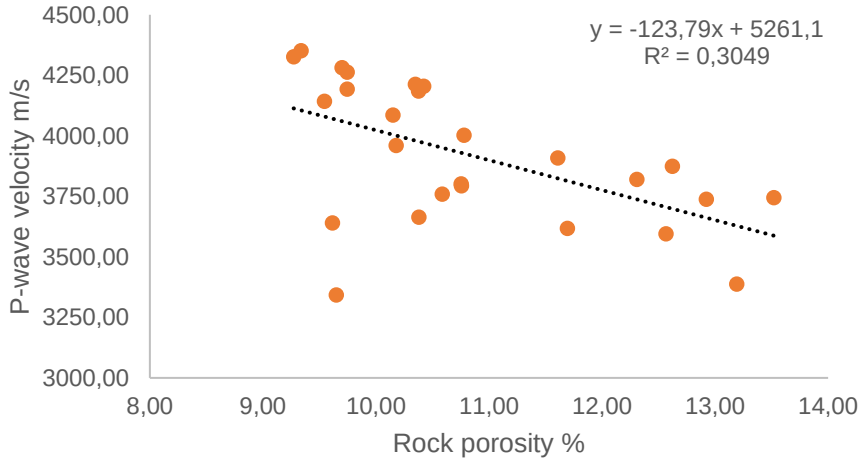

Figure 40 - P-wave velocity Vs Rock porosity measured with water

Analysing the previous results, P-wave velocities are between 3000-4000 m/s range. Core samples from number 15 to 20 present abnormal results in comparison to the rest of the samples. It could be related to the fact that these samples were cut from different locations of the main rock in comparison to sample 1 to 14, thus possibly presenting different characteristics.

From Figure 39 it was noticed that low P-waves velocities were associated to low values of density, however there is a high variation on the results and the coefficient of determination is very low (R^2 = 0,3404) not being possible to guarantee a relation between both properties. These oscillations could be related to the heterogeneities of the rock, pore size, different compositions or other properties that are not macroscopically visible.

When analysing water saturated core samples (Figure 40), the same range of velocity values was presented, 3000-4000m/s and low P-waves velocities were associated to high porosity values. For this case it was also noticed a high oscillation on the values making it hard to relate both properties (R^2 = 0,3049). Until sample 14, core samples presented higher values of velocity compared to dry core samples. After that the opposite happens, this effect could be related to rock heterogeneities. Overall, they present the same behaviour (Table 30).

In conclusion, the wave velocity with high porosity rocks completely saturated with water is lower than in lower porosity rocks, because the P-wave velocity in water is smaller than the P-wave velocity in mineral skeleton as stated by Gregory et al. and Lama and Vutukuri. [31, 75-77]

When changing the saturation fluid, the following results were obtained.

Table 12 - Measurements and P-wave velocity results for saturated core samples

Core samples	Core length (mm)	Density (kg/m^3)	Rock Porosity %	Saturated core velocity (m/s)	Saturation Fluids
1	90,57	2373,60	10,35	4193,06	Brine
2	90,57	2389,91	9,75	4252,11	Isooctane
3	90,47	2299,63	12,92	3882,83	Isooctane
4	90,62	2293,24	13,52	4195,37	Brine
6	90,47	2301,81	13,19	3662,75	Hexadecane
8	90,47	2362,72	10,78	4075,23	Dodecane
9	90,53	2395,35	9,34	4416,10	Isooctane
11	90,66	2389,35	9,61	4177,88	Isooctane
12	90,29	2311,05	12,62	3977,53	Isooctane
13	90,62	2367,90	10,59	3957,21	n-Octane
14	90,67	2362,55	10,76	4084,23	Hexadecane

The overall results are the same however, with an increase in all velocities (better seen on Table 13) when the core is saturated with hydrocarbons. It was then compared all the velocity scenarios in the following table:

Table 13 - Dry and saturated core samples P-wave velocity

Core samples	Dry core P-wave velocity (m/s)	Water saturated core P-wave velocity (m/s)	Brine saturated core P-wave velocity (m/s)	Hydrocarbon saturated core P-wave velocity (m/s)
1	3681,79	4212,65	4193,06	-
2	3652,18	4193,24	-	4252,11
3	3301,97	3738,60	-	3882,83
4	3307,37	3744,71	4195,37	-
6	3119,52	3388,24	-	3662,75
8	3520,08	4002,92	-	4075,23
9	3725,60	4352,50	-	4416,10
11	3320,73	3640,80	-	4177,88
12	3356,43	3875,02	-	3977,53
13	3356,22	3760,08	-	3957,21
14	3555,84	3793,89	-	4084,23

When comparing the results of all the different saturations, it is possible to see that there is an increase in velocity as the saturation fluid is changed. It was shown through Biot's theory and Gassmann's equation that P-wave velocity increases when a porous media is saturated with a liquid [33]. It is difficult to state that the values of velocity are what is expected because carbonate rocks present different conditions, porosity, heterogeneities, pore size and faults therefore, different ranges of velocities according to these characteristics can be obtained.

According to Wang, Z et al. (1991) [32], P-wave velocity increases due to a decrease in compressibility. Which means, when the air in the pores is replaced by a much less compressible fluid, oil in this case, the compressibility of pores decreases drastically thus, decreasing the overall compressibility of the core.

The difference between P-wave velocities of water and hydrocarbons saturated cores is very little, however, in theory, cores saturated with water should have presented higher velocity comparing to hydrocarbon saturated cores since water is less compressible than oil. Again, these results could be related to rock heterogeneities.

Some researchers have investigated the effect of porosity in P-wave velocity and concluded that exists an inverse relation [74, 78]. Oliveira et al. (2016) [78] studied outcrops of carbonate rocks from different regions and plotted the relation between porosity and Vp (Figure 41).

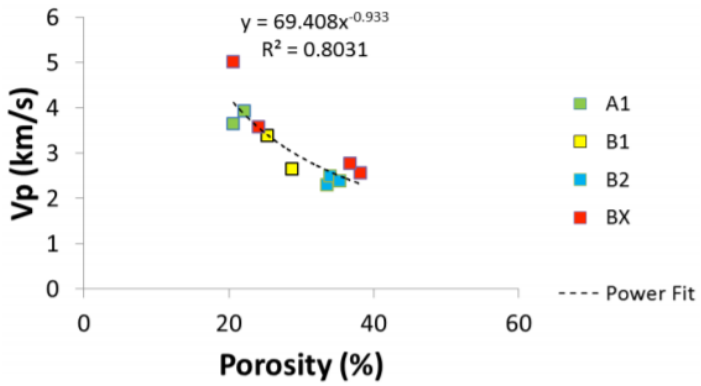

Figure 41 - Cross plot of Porosity and P-wave velocity (Vp). The dashed line shows the best fit. [78]

4.3 Hydrocarbon Recovery

After the core porosity and permeability analysis was concluded and seismic tests performed, the next step was to start hydrocarbon flow throughout the rock sample to determine its absolute permeability and further step into the binary mixtures flow.

4.3.1 Hydrocarbon Absolute Permeability Analysis

Here, the samples were saturated with each hydrocarbon isooctane, hexadecane, n-octane and dodecane, individually. As mentioned before and to guarantee the assumptions previously made about porosity and permeability relation, several cores were tested with higher and lower porosity to predict if the permeability values would correspond to these variations. More samples were tested with Isooctane because it was the hydrocarbon with lower viscosity and the one who could present better results. (Table 14, Table 15)

The tests were performed with the same conditions mentioned before for the brine permeability procedure. The confining pressure was 50 bar, and the injection flow rate was 3mL/h and 6mL/h. On Table 15 the absolute permeability was calculated with an injection flow rate of 6mL/h.

Table 14 - Characterization of cores applied in synthetic hydrocarbons recovery

Core Samples	Average Diameter (mm)	Average Length (mm)	Dry weight (g)	Mass after saturation (g)	Saturation Fluid
2	37,88	90,57	243,99	251,15	Isooctane
3	37,93	90,47	235,05	244,97	Isooctane
6	37,90	90,47	234,88	246,71	Hexadecane
8	37,85	90,47	240,46	249,09	Dodecane
9	37,90	90,53	244,69	251,59	Isooctane
11	37,91	90,66	244,54	251,89	Isooctane
12	37,87	90,29	235,07	245,02	Isooctane
13	37,90	90,62	241,78	250,31	n-Octane
14	37,89	90,67	241,59	250,45	Hexadecane

Table 15 - Hydrocarbon porosity and absolute permeability

Core Samples	Water porosity %	Hydrocarbon Porosity %	Absolute Permeability mD	Saturation Fluid
2	9,75	10,11	0,053	Isooctane
3	12,92	14,02	0,138	Isooctane
6	13,19	14,98	0,200	Hexadecane
8	10,78	11,36	0,065	Dodecane
9	9,34	9,76	0,022	Isooctane
11	9,61	10,73	0,036	Isooctane
12	12,62	14,38	0,174	Isooctane
13	10,59	11,93	0,077	n-Octane
14	10,76	11,57	0,075	Hexadecane

Analysing each hydrocarbon at the time, for Isooctane five tests were made. Three of them had rock porosities in the range of 9-10% and the remaining two approximately 13%. The porosities of the hydrocarbons are similar to the rock porosity determined with water however, the hydrocarbons present higher values because their interaction with the rock is easier. Regarding to the permeability, for lower porosities it was obtained lower permeability values when compared to the values obtained with higher porosity. So, the assumption made before confirms with the values obtained now.

This effect happens for the remaining hydrocarbons, hexadecane, dodecane and n-octane. For lower porosity values it is obtained lower permeability values. Between hydrocarbons with similar rock

porosities, the permeability values are very similar. For example, considering low porosities, sample 2 (isooctane), 8 (dodecane), 13 (n-octane) and 14 (hexadecane) present 0,053 mD, 0,065 mD, 0,077 mD, and 0,075 mD, respectively. Which means that besides the molecular weight, density, viscosity, polarizability and molecule linearity, the permeability values are not too different.

It is also important to notice that the permeability of these hydrocarbons is also similar to the brine permeability analysed before, 0,069 mD considering low porosities (Table 11). Summing up, this carbonate rock seems to produce the same results, for the same porosity range, regardless of the displacement fluid type.

To analyse this phenomenon, a graph was made directly comparing the values of the rock porosity and hydrocarbons permeabilities.

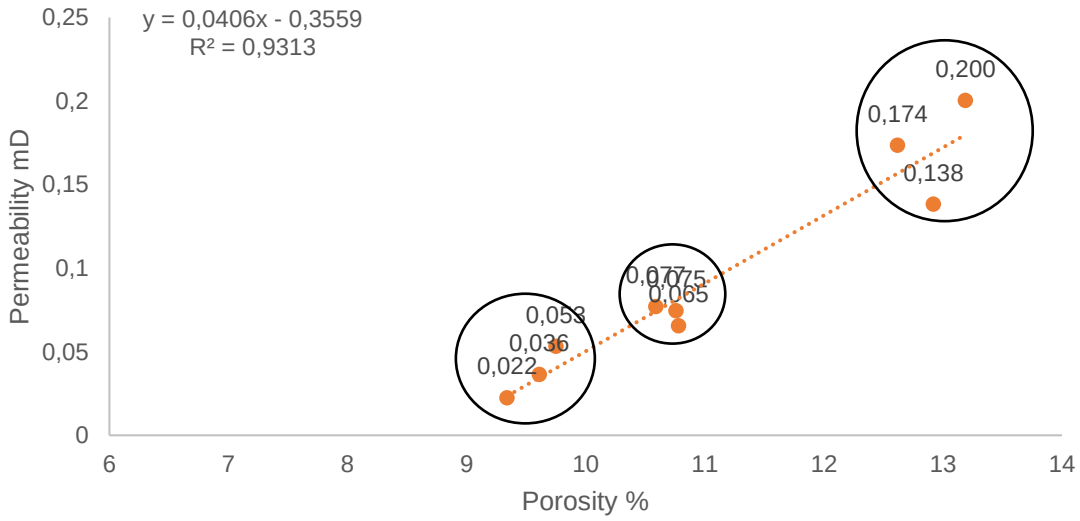

Figure 42 - Rock porosity Vs Hydrocarbons permeabilities

It is possible to notice three clusters of values. The first one includes the values of permeabilities lower than 10% porosity, second one permeabilities with porosities between 10-12% and lastly permeabilities with porosity values higher than 12%. According to the graph, the high coefficient of determination (0,9313), proves that in fact exists a relation between these properties. Samples with porosities in the last cluster were preferred because it reproduced the expected results from the previous thesis of Pinto (2020) [54].

4.3.2 Binary Oil Mixtures Permeability Analysis in Carbonate Rock

After analysing hydrocarbons single permeabilities, it was time to explore the permeability of hydrocarbons mixtures and its behaviour. The study of binary oil mixtures flow had as main objective the analysis on how the proportion of hydrocarbons can influence in final permeability results. The hydrocarbons oil mixtures considered were isooctane / n-octane and isooctane / dodecane (for multiple proportions) and the final results are expressed on Table 16.

Table 16 - Rock and hydrocarbon Porosity, absolute permeability for isooctane/dodecane and Isooctane / n-Octane mixtures

	70% Isooctane / 30% Dodecane	70% Isooctane / 30% Dodecane	70% Isooctane / 30% n-Octane	50% Isooctane / 50% n-Octane	30% Isooctane / 70% n-Octane
Rock Sample #	18	5	10	7	22
Rock Porosity %	12,31	10,38	10,38	10,15	10,75
Hydrocarbon Porosity %	15,46	12,12	10,74	10,72	11,98
Absolute Permeability mD	0,0163	0,025	0,033	0,053	0,078

According to the results, it is possible to see that for Isooctane / Dodecane mixture, only two samples (#5 and #18) were used with the same hydrocarbon proportion, varying only its porosity values. Sample #5 with lower porosity obtained a lower permeability result when comparing to sample #18 which presented a higher porosity.

It was previously observed that porosity had an impact in permeability values for single fluid flow. Now, using mixtures, it is possible to see that this influence is consistent, therefore, for lower porosity it is expected a lower permeability regardless of the injection/saturation fluid.

For Isooctane / n-Octane mixtures, three samples were used (#7, #10 and #22) with different hydrocarbon proportions. As the quantity of n-Octane increased over the essays, it was noticed an increase in the permeability of the mixtures as well. So, for 70-30, 50-50 and 30-70 proportions the permeability was 0,033 mD, 0,053 mD and 0,078 mD, respectively. In addition, the samples were carefully chosen (similar porosity) to guarantee that this phenomenon was not related to other external property influence.

The increase of flow and permeability is often related to the increase of the percentage of lighter components. Pinto (2020) [54] observed that for isooctane / dodecane mixtures since it was analysed multiple proportions.

Regarding to Isooctane / n-Octane, n-Octane presents a higher density than Isooctane, therefore it is a heavier component. When analysing these two hydrocarbons C_8H_{18}, the main property that distinguish

them it is its structures (Figure 30) since isooctane is an isomer of n-Octane. Isooctane is a branched hydrocarbon and n-Octane has a linear structure, which means that isooctane presents a higher kinetic diameter when compared to n-Octane. With that being said, it is more likely for the increase of permeability on this mixture to be related to the kinetic diameter influence, which enables the flow of lower kinetic diameter hydrocarbons in comparison with higher ones.

4.3.3 Differential Permeability Analysis in Carbonate Rock

Until now it was already analysed carbonate's rock properties (porosity and permeability), seismic test to understand the variation of P-wave velocity and hydrocarbons permeability of single flow and homogeneous mixtures. The following step is the analysis of how homogeneous mixtures of hydrocarbons crosses a carbonate rock and examine if there is a preference on the flow of these mixtures.

For that, the effluent collected from the previous cores (Table 16), with isooctane / dodecane and isooctane / n-Octane mixtures, was used and analysed in the gas chromatograph.

On Pinto (2020) [54] the hydrocarbon mixtures were isooctane / dodecane and isooctane / hexadecane and since one of the objectives was to compare results, it was important to choose at least one of the mentioned mixtures to validate the obtained results. The second mixture isooctane / n-octane was chosen because it would be interesting to analyse the flow of two C_8 hydrocarbons (isooctane is any isomer of n-octane). On Table 17 is expressed the characteristics of the chosen cores.

Table 17 - Characterization of cores applied in differential permeability analysis for Isooctane / Dodecane mixture

Core Samples	Average Diameter (mm)	Average Length (mm)	Dry weight (g)	Mixture mass after saturation (g)	Rock Porosity %	Mixtures % Isooctane / Dodecane
5	37,93	90,39	241,16	249,96	10,38	70/30
18	37,70	100,85	263,67	274,87	12,31	70/30

The core flooding experiment to determine differential permeability was performed for approximately 3 hours and the effluent fluid was collected every five minutes for two hours in polytopes. After that, the fluid was inserted in the gas chromatograph to analyse its composition and assess if the 70/30 proportion maintains. On Figure 43 and Figure 44, the points refer to the percentage of each compound in the effluent provided by the Gas Chromatograph.

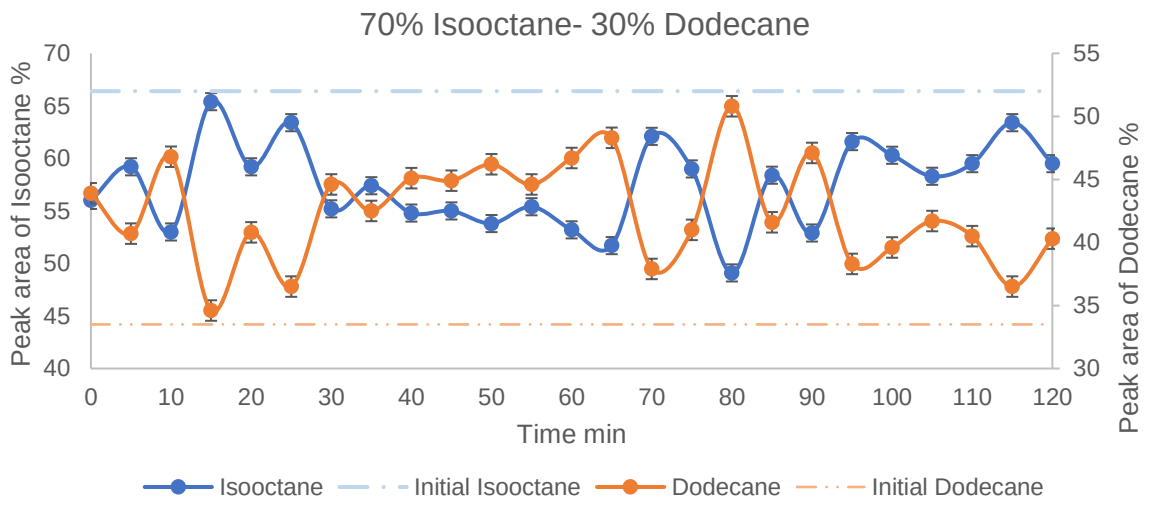

Figure 43 - Differential Permeability of 66,4% Isooctane / 33,6% Dodecane mixture – Core 5

For Core 5, which initial composition was 66,4% of Isooctane and 33,6% of Dodecane it was noticed a preference of dodecane flow in the beginning of the experiment, being the percentage measured in the first drop collected of 56,1% / 43,9%. After that there were multiple oscillations of preferential flow but, there was a preference of Isooctane until the end of the experiment. It was also possible to notice that the range of values was very big for isooctane and dodecane percentages being 49% the lowest value and highest 66% for isooctane and 34% the lowest value and highest 51% of dodecane.

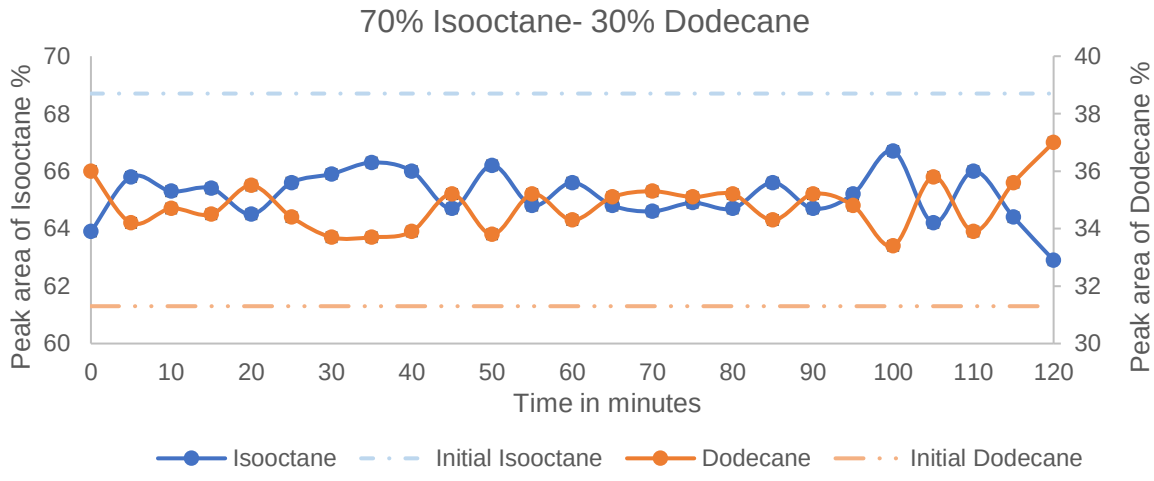

Figure 44 - Differential Permeability of 68,7% Isooctane / 31,3% Dodecane mixture – Core 18

For core 18, which initial composition was 68,7% Isooctane and 31,3% Dodecane also presented a preference, on the beginning of the experiment, for dodecane being the first drop of fluids proportion of 64%-36%. Throughout the rest of the test the proportion of the mixtures presented an alternate preferential flow, however the percentage of isooctane was always higher than the proportion of

dodecane. The range of values for this experiment for Isooctane was shorter compared to the previous one, being the lowest value of isooctane 64% and the highest of 67%. Correspondingly, dodecane's lowest value was 33% and higher 36%.

Summarising, for both rock samples with isooctane / dodecane mixture, it was observed a higher percentage of isooctane in the entire experiment (regardless of the alternated flow).

Isooctane is a branched hydrocarbon when compared to dodecane which is a straight chain alkane [79]. In addition, isooctane presents a higher kinetic diameter of 6,2 Å while dodecane has 4,6 Å [80] and its structure is represented on Figure 45 (obtained through a molecular simulation program). When imagining a pore structure, it is possible that a preference of dodecane flow happens since not only presents a lower kinetic diameter but also is a linear hydrocarbon. However, one can also take into consideration that isooctane is an overall smaller molecule and has a lower dynamic viscosity.

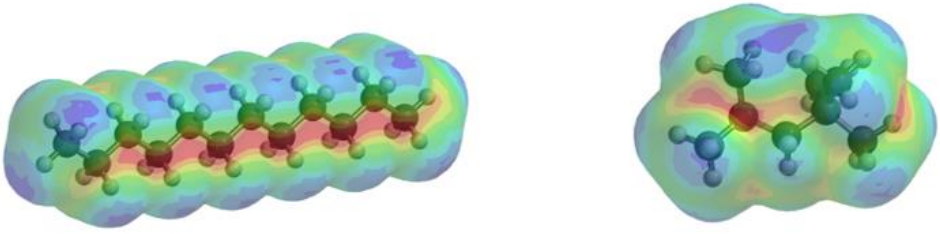

Figure 45 - a) Dodecane structure; b) Isooctane structure

This experiment was performed for two different cores with different porosities to see how the porosity could affect the distribution of the homogenous mixture during the flow and, subsequently, the differential permeability. Core 5 presented a porosity of 10,38% while core 18 presented 12,31% (Table 17). The hydrocarbons behaviour was similar in both core samples regarding to the preferential flow variability. However, it was possible to notice that the range of values on the first experiment was higher than the values of the second one. Which means that, for the first sample, a higher quantity of isooctane is held and consequently allows a higher quantity of dodecane to cross the rock sample. For the second sample, with higher porosity, there is a smaller quantity of isooctane retained.

Since it was not possible to analyse the pore structure it is not viable to affirm that a low porosity means that the size of the pores is smaller. Still, it is a possibility that with a higher kinetic diameter and a lower porosity it is more likely for the hydrocarbons to be kept from crossing the rock sample, enabling the hydrocarbons with lower kinetic diameter and linear structure to cross the rock specimen. Concluding, a higher porosity implies a lower differential permeability which means that there is a more balanced flow of hydrocarbons throughout the rock sample.

Along the experiment some hydrocarbons may be kept inside the rock sample, being the mass of each component before the assay different of the mass at the end. Given this, a mass balance was made to quantify the amount of each component in the core sample. The mass of each component introduced during the assay is:

$$m_{mist} = Q_P \times \rho_{mist} \times t \quad \text{(Eq.17)}$$

$$m_{X\,int} = m_{mist} \times \%\, x_i \quad \text{(Eq.18)}$$

Where m_{mist} represents the mixture mass introduced (g), Q_P is the flow provided by the injection pump (mL/h), ρ_{mist} is the density of the mixture (g/cm^3) and, t is the pump operating time (h). Also, $m_{X\,int}$ is the component mass introduced (g) and $\%x_i$ is the initial component percentage.

Regarding to the collected mass, it was calculated using the measured effluent mixture mass over the time of the procedure and the percentage of each component provided by the gas chromatograph, shown in the previous graphs.

$$m_{X\,j} = m_{mist\,j} \times \%\, x_j \quad \text{(Eq.19)}$$

$$m_{X\,col} = \Sigma\, m_{x\,j} \quad \text{(Eq.20)}$$

With $m_{x\,j}$ the component mass collected during j interval of time (g), $m_{mist\,j}$ is the mixture mass collected during j interval of time (g), $\%x_j$ is the component percentage in j interval of time and, finally, $m_{X\,col}$ is the total component mass collected (g).

In addition, the core was analysed before and after the experiment using the following equations:

$$m_{X\,initial} = m_{mixt\,i} \times \%x_i \quad \text{(Eq.21)}$$

$$m_{X\,final} = m_{xi} + m_{x\,int} - m_{x\,col} \quad \text{(Eq.22)}$$

Where $m_{X\,initial}$ is the initial component mass in the core (g), $m_{mixt\,i}$ is the initial mass of the mixture in the core, introduced after the saturation process (g) and, $m_{X\,final}$ is the final component mass (g).

On Table 18 is represented the mass balance for both core samples with Isooctane / Dodecane homogeneous mixture.

Table 18 - Isooctane / Dodecane - Mass balance

Core Samples	Rock Porosity %	Introduced Mass %		Collected Mass %	
		Isooctane	Dodecane	Isooctane	Dodecane
5	10,38	66,4	33,6	59,5	40,3
18	12,31	68,7	31,3	62,9	37,1

For the second mixture, Isooctane / n-Octane, three different proportions were used 70/30, 50/50 and 30/70 and the experiment was conducted with the same conditions as the previous mixture which means, the effluent fluid was collected every five minutes for 2 hours in polytopes and the total essay duration was approximately 3 hours. The core samples used are characterized on the table below.

Table 19 - Characterization of cores applied in differential permeability analysis for Isooctane / n-Octane mixture

Core Samples	Average Diameter (mm)	Average Length (mm)	Dry weight (g)	Mixture mass after saturation (g)	Rock Porosity %	Mixtures % Isooctane / Dodecane
10	37,92	90,50	242,34	249,97	10,38	70/30
7	37,88	90,31	242,66	250,29	10,15	50/50
22	37,88	91,61	244,37	252,91	10,75	30/70

On the following figures are presented the flow of Isooctane / n-Octane mixtures for different proportions. Again, the points refer to the percentage of each compound in the effluent provided by the gas chromatograph.

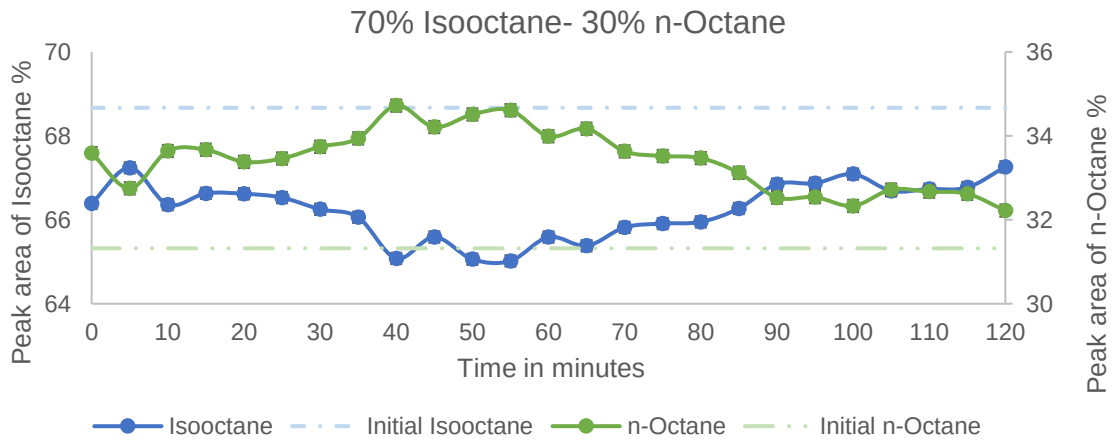

Figure 46 - Differential Permeability of 68,7% Isooctane / 31,3% n-Octane mixture – Core 10

For core 10, the initial composition was 68,7 % of Isooctane and 31,3% of n-Octane before the experiment has started. On the first drop of fluid the measured isooctane percentage dropped to 66,4% and subsequently n-octane percentage increased to 33,6%. This shows that a preferential flow of n-octane happened. During the rest of the experiment until minute 65 it was noticed a continuous alternated flow of isooctane and n-octane. Between minute 65 and 100 a gradual increase of isooctane could be observed. From minute 100 to 120 the flow was once again alternated. However, the percentage of isooctane was always higher than n-octane throughout the experiment.

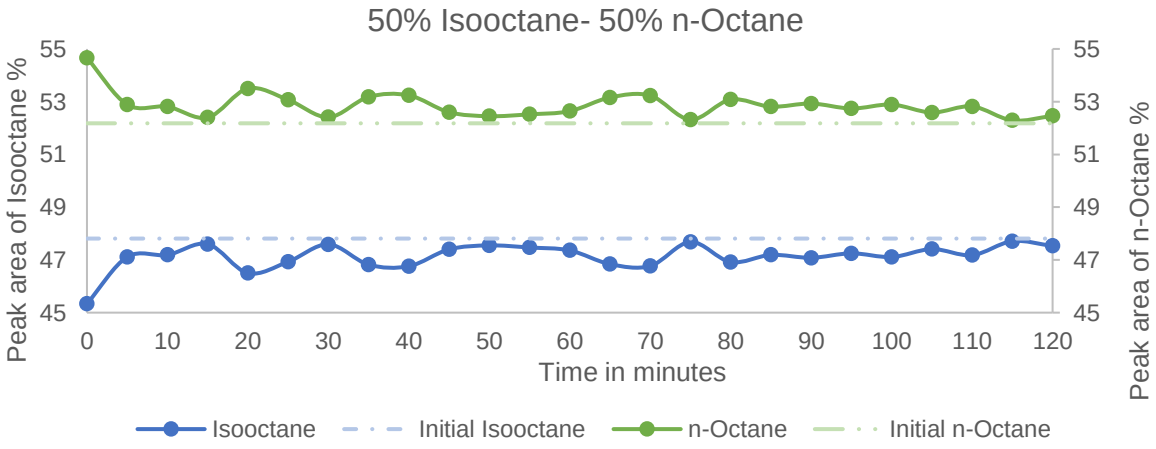

Figure 47 - Differential Permeability of 47,8% Isooctane / 52,2% n-Octane mixture – Core 7

For core 7, the initial composition measured was 47,8% of Isooctane and 52,2% of n-Octane. The first drop collected indicated once again a preferential flow of n-octane since the percentages were 45,3% isooctane / 54,66 % n-octane. For this mixture proportion, a more alternated flow was noticed, not being

detected a continuous decrease, or increase of neither component. Here, the percentage of n-octane was always higher than isooctane's throughout the experiment.

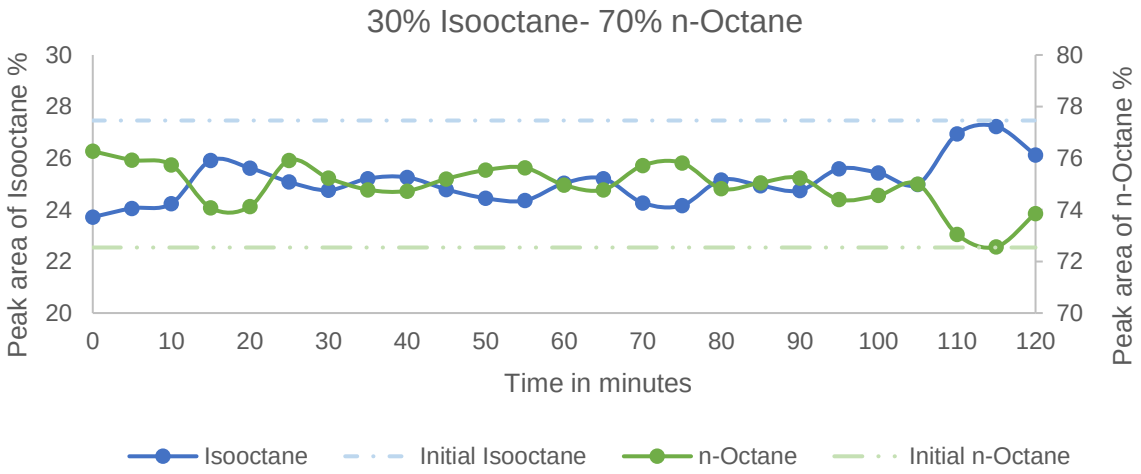

Figure 48 - Differential Permeability of 27,5% Isooctane / 72,5% n-Octane mixture – Core 22

For core 22, which initial percentage was 27,5% of Isooctane and 72,5% of n-Octane a preferential flow of n-octane was observed as expected since the first drop's percentage indicated 23,7% isooctane / 76,3% n-octane. The flow was alternated along the essay and the percentage of n-octane was always higher.

Summing up, for all the cores with different mixture compositions, the flow was alternated and an initial preference for n-octane was observed.

The objective here was to analyse how different hydrocarbons behaved when crossing a carbonate sample. As mentioned before, isooctane molecules present a kinetic diameter of 6,2 Å while n-octane has 4,5 Å [80] and its structure is represented below (obtained through a molecular simulation program).

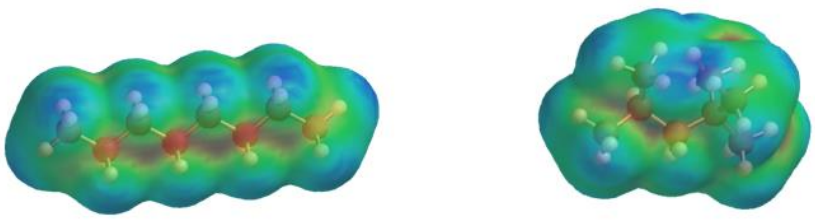

Figure 49 - a) n-Octane structure; b) Isooctane structure

Given this, and having core samples with similar characteristics (porosity, dimension, etc), it is possible to notice that the kinetic diameter had an influence on the flow of these mixtures since there was always a preference for n-octane on the first drop. Also, for the 50-50 proportion, n-octane presented always higher percentages.

For Isooctane / n-Octane mixtures, a mass balance was also performed (Table 20), which reaffirms the preferred flow for n-Octane in all essays.

Table 20 - Isooctane / n-Octane - Mass balance

	Rock Porosity %	Introduced Mass %		Collected Mass %	
		Isooctane	n-Octane	Isooctane	n-Octane
10	10,38	68,7	31,3	67,3	32,2
7	10,15	47,8	52,2	47,5	52,5
22	10,75	27,5	72,5	26,1	73,9

4.4 Comparison of Results: Carbonate rock Vs Sandstone rock

It was mentioned multiple times throughout this research that one of the main objectives was to compare results with a former work developed on carbonates and sandstones [54]. However, the same rock properties were determined but, not all of them on the same way since carbonate rocks and sandstone rocks present different characteristics and endurance.

4.4.1 Porosity

The sandstone porosity was measured in three different ways for five different fluids (water, brine, isooctane, dodecane and hexadecane), the first essay the specimen was saturated for 18 hours (Assay #1), the second one the sandstone was vacuumed for 2 hours (Assay #2) and finally, the sample was saturated and heated (80°C) for 2 hours (Assay #3). The results are depicted bellow.

Table 21 - Sandstone porosity (%) [44]

Assay	Water	Brine (35 g/L of NaCl)	Isooctane	Dodecane	Hexadecane
#1	30.2	29.5	35.0	34.8	35.2
#2	37.5	37.5	39.6	40.1	40.0
#3	39.7	38.8	38.8	40.3	39.9

For carbonate rock porosity results for water, brine, isooctane, dodecane, hexadecane and n-octane were:

Table 22 - Carbonate porosity (%)

Core samples	Water (%)	Brine (%)	Isooctane (%)	Dodecane (%)	Hexadecane (%)	n-Octane (%)
1	10,35	10,64	-	-	-	
2	9,75	-	10,11	-	-	
3	12,92	-	14,02	-	-	
4	13,52	13,34	-	-	-	
5	10,38	-	-	-	-	
6	13,19	-	-	-	14,98	
7	10,15	-	-	-	-	
8	10,78	-	-	11,36	-	
9	9,34	-	9,76	-	-	
10	10,38	-	-	-	-	
11	9,61	-	10,73	-	-	
12	12,62	-	14,38	-	-	
13	10,59	-	-	-	-	
14	10,76	-	-	-	11,57	

Comparing the results, it is possible to see a substantial difference between the values. Sandstone porosity is massively higher compared to carbonate porosity, as expected. However, it is important to say that the sandstone rock was disaggregated which enhanced the sample porosity. On the other hand it is also possible to see similarities in the behaviour of the samples.

Sandstone water and brine porosity are very close regardless of the saturation process. For carbonates samples the same happens being the difference in porosity lower than 1% between water and brine.

For isooctane a bigger difference in porosity is noticed for both rock specimens. However, it is also visible that for rock samples with lower porosity the difference between fluids porosity (water vs isooctane) is not that accentuated when compared to specimens with higher porosity. In other words, the higher the porosity of the rock, the higher the difference between fluids porosity, and this applies for all hydrocarbons.

In conclusion, sandstone is more porous than carbonates but, increasing water salinity and increasing oil molecular weight, by using heavier hydrocarbons, does not change the amount of porous media available.

4.4.2 Absolute Permeability

For permeability measurements water, brine, and hydrocarbons (absolute and differential) were also used for sandstone rock. For carbonate rock the same tests were performed, with exception of water, and the results are as follows:

Table 23 - Overall sandstone permeability [54]

Hydrocarbons	Permeability (mD)	% Isooctane / % Dodecane	Permeability (mD)	% Isooctane / % Hexadecane	Permeability (mD)
Isooctane	8143.7			88.2 / 11.8	7924.4
		69.6 / 30.4	5776,7		
Octane	7885.2			70.5 / 29.5	4284.0
		47.9 / 52.1	5554.5	49.0 /51.0	4221.0
Dodecane	2737.4				
				30.3 / 69.7	3868.4
		31.4 / 68.6	4472.7		
Hexadecane	2300.9			10.9 / 89.1	2501.8
Water	220.3	Brine	488.6		

Table 24 - Overall carbonate permeability

Core Samples	Absolute Permeability (mD)	Saturation Fluid
1	0,069	Brine
2	0,053	Isooctane
3	0,138	Isooctane
4	0,116	Brine
6	0,200	Hexadecane
8	0,065	Dodecane
9	0,022	Isooctane
11	0,036	Isooctane
12	0,174	Isooctane
13	0,077	n-Octane
14	0,075	Hexadecane

Sandstone's permeability results are by far higher than carbonate rocks, which was the expected since the sandstone rock was disaggregated and presented easier conditions for fluid flow. In the previous chapters it was mentioned a relation between porosity and permeability, and it was assumed that for a higher porosity it would be more likely to achieve a higher permeability. Here the same happened. Sandstone rock samples porosity was in the range of 30-40% while carbonated were between 9-14%, which enabled a higher permeability for the sandstone samples and lower for carbonates. This conclusion is reflected in sandstone vs carbonate results and carbonates with low porosity vs carbonates with higher porosity results.

Besides the values, it is also important to evaluate the behaviour of the permeability when the fluids are changed. For sandstones it was observed that as the molecular weight of hydrocarbons increase, a permeability reduction occurs, decreasing three times when the number of carbon atoms in the oil increases from 8 to 12. When number of carbon atoms increase from 12 to 16 the reduction is smaller.

For carbonates the opposite happens. When comparing oil permeabilities of rock samples with similar porosities (to eliminate some variability), it is possible to see that with an increase of the molecular weight of hydrocarbons, permeability values are enhanced (samples 2, 8, and 14). However, the difference between these values is not too relevant ($\pm\ 0{,}022\ \mathrm{mD}$) since they present more or less similar values of permeability, even for brine.

To best discuss these results, an analysis of kinetic diameter effect on fluid flow was performed. As mentioned, kinetic diameter is a measure applied to atoms and molecules that expresses the size of a molecule. Hydrocarbon structures are presented on Figure 50, obtained through a computational program (Spartan).

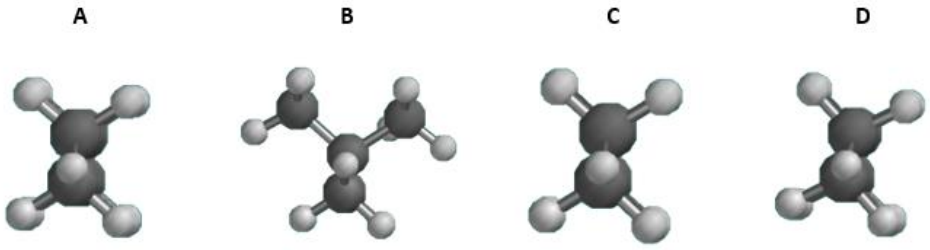

Figure 50 – Frontal view of n-octane (A), Isooctane (B), n-Dodecane (C) and n-Hexadecane (D).

According to Jiménez-Cruz [80], isooctane presents a higher kinetic diameter of 6,2 Å while dodecane has 4,6 Å and n-octane 4,5 Å. Ahmed et al. [81], stated that like other n-alkanes, n-hexadecane presents a diameter of 4,6 Å. The order of magnitude from the lowest kinetic diameter is n-octane, n-hexadecane, dodecane and isooctane.

When associating these values to permeability results, a high influence of kinetic diameter can be observed because with an increase of kinetic diameter, for branched hydrocarbons (isooctane) the permeabilities decrease and, for a decreased kinetic diameter an increase permeability occurs. As mentioned in chapter 24, for C_{15+} alkanes, the lower molecular weight components undergo migration more readily than higher molecular weight components and n-alkanes migrate faster than branched alkanes (Leythaeuser et al. (1983) [42]).

While this phenomenon occurs for carbonates, the opposite occurs for sandstones thus, sandstones pore network is probably composed by macro pores while carbonates pore network is smaller being kinetic diameter's influence more relevant.

4.4.3 Binary oil mixtures permeability analysis

In the previous thesis, sandstones binary oil mixtures permeabilities were also analysed. The objective here was to observe how the influence of different percentages of each compound had an effect on mixtures permeabilities. The first table is related to sandstones overall permeabilities (for each compound, mixture water and brine) and the second to carbonates.

Table 25 - Overall sandstone's permeabilities [54]

Table 4.3 – Overall permeabilities.

Hydrocarbons	Permeability (mD)	% Isooctane / % Dodecane	Permeability (mD)	% Isooctane / % Hexadecane	Permeability (mD)
Isooctane	8143.7			88.2 / 11.8	7924.4
		69.6 / 30.4	5776,7		
Octane	7885.2			70.5 / 29.5	4284.0
		47.9 / 52.1	5554.5	49.0 /51.0	4221.0
Dodecane	2737.4				
				30.3 / 69.7	3868.4
		31.4 / 68.6	4472.7		
Hexadecane	2300.9			10.9 / 89.1	2501.8
Water	220.3	Brine	488.6		

Analysing only the mixtures permeabilities values, they are inside the range of pure hydrocarbons permeabilities compounds, discussed on the previous chapter and, the mixtures permeability increases with higher isooctane percentage (for both mixtures).

Table 26 - Carbonate´s mixtures permeabilities

Hydrocarbon's mixtures	Absolute Permeability (mD)
70% Isooctane / 30% Dodecane	0,025
70% Isooctane / 30% Dodecane	0,163
70% Isooctane / 30% n-Octane	0,033
50% Isooctane / 50% n-Octane	0,053
30% Isooctane / 70% n-Octane	0,078

When comparing to Table 24, mixture permeabilities values are also inside the range of pure hydrocarbons permeabilities. It is also possible to see that permeability values increase with smaller quantities of isooctane and higher of n-octane percentages.

It was expected to see that, sandstones binary oil mixtures permeabilities would be higher than carbonates binary oil mixtures permeabilities, as it was discussed on previous chapters. However, for this first rock sample the behaviour was for permeability increase with higher isooctane, and for carbonates the permeability increases with lower isooctane. This effect happens for the sandstones because isooctane in comparison with dodecane and hexadecane has lower molecular weight thus, its flow is enabled, even though isooctane has a higher kinetic diameter when compared to hexadecane and dodecane.

For carbonates, the mixture is isooctane and n-Octane, and it was already analysed that isooctane is an isomer of n-Octane and the main difference is the molecular structure. Isooctane being a branched hydrocarbon creates more difficulty flowing through carbonates porous since they are smaller (when compared to sandstones), enabling the flow of n-Octane, linear hydrocarbon. Therefore, permeability increases when n-Octane increases.

Summarizing, permeability increases with the increase of lower molecular weight compounds or when the kinetic diameter of the compound with higher percentage is lower. However, the effect of the kinetic diameter is more evident when dealing with smaller pore sizes.

4.4.4 Differential permeability analysis for mixture injection

Differential permeability analysis was performed for both rock samples. The objective was to analyse how homogeneous oil mixtures flow through a core sample and examine the fluid composition before and after the essay. The only common mixture for both rock samples was isooctane / dodecane with a 70%-30% proportion, respectively.

For sandstone core sample a mixture of 69,7% Isooctane / 30,3% Dodecane was obtained (Figure 17a). During the first hour it was noticed in the outlet stream an increase in the amount of Isooctane. After that, the amount of dodecane increased although in the end of the assay the amount of isooctane started to increase again. The percentage of Isooctane was always higher than the percentage of Dodecane throughout the experiment.

For carbonate core sample (Figure 44) a mixture of 68,7% Isooctane / 31,3% Dodecane was obtained. In the beginning of the assay, it was noticed an increase in Dodecane (minute 0), but it was rapidly shifted to an increase of Isooctane in the first 10 min. After that it was observed an alternated decrease and increase in Isooctane throughout the experiment. Again, the percentage of Isooctane was always higher than the percentage of Dodecane.

In both experiments, besides the different assay time, it was found an alternate preferential flow of Dodecane and an overall higher percentage of Isooctane along the test. These results show that even though the mixtures are homogeneous, their components do not flow homogeneously. The mass balance is represented on Table 27.

Table 27 - Mass balance at Isooctane / Dodecane mixtures

	Introduced Mass (%)		Collected Mass (%)	
	Isooctane	Dodecane	Isooctane	Dodecane
Sandstone	69,7	30,3	69,5	30,5
Carbonate	68,7	31,3	62,9	37,1

For sandstone sample it was noticed a higher percentage of isooctane at the end of the test when compared to the carbonate sample, which was expected. Since the sandstone was considered to be composed by macro pores, it allows a higher quantity of hydrocarbons to flow with higher kinetic diameters.

On the other hand, carbonate samples are composed by smaller pores when compared to sandstones which could have an influence in branched hydrocarbons (isooctane) flow. Thus, carbonate samples may enable a preferential flow of linear hydrocarbons (dodecane) as mentioned on chapter 4.3.3.

5. Conclusion and Future Work Suggestions

On this final chapter, it is presented a brief summary and the main conclusions discussed on this research along with some future work suggestions and possible improvements.

5.1 Conclusion

After the carbonate rock acquisition from the Maciço Calcário Estremenho region, it was possible to characterize the specimen's properties such as porosity and permeability (with water, brine, and hydrocarbons), with aid of the core flooding system. Also, an important analysis of the P-waves velocity through a saturated and dry core was accomplished. After that, a more thorough analysis was performed for hydrocarbons flow and its properties (structure, molecular weight, kinetic diameter) influence when crossing a rock sample, and a comparison between sandstones and carbonates properties was made.

The carbonate sample porosity, measured with water, presented values in the range of 9,27% to 13,52%, being the majority below 10%, which corresponded to the average porosities usually found in carbonate rocks (5-15%). However, the porosity values were expected to be higher since Codaçal rocks present values between 11,2% and 12,8%. This low porosity could be associated to less or fractured pores.

Regarding the carbonate permeability, measured with brine, the rock analysis was performed for constant confining pressure, different porosity samples and different flow rates (3mL/h and 6mL/h). The values varied from 0,022 to 0,069 mD for low porosity samples and from 0,116 to 0,128 mD for high porosity samples. It was possible to observe an impact of the porosity in permeability results since low porosity samples were associated to low permeabilities and high porosity samples to high permeabilities. Regarding to the flow rate variability, it was noticed a slight alteration on the values however, it did not have a relevant influence.

P-waves velocity analysis was also performed for dry and saturated carbonates samples in order to analyse how P-waves behave in different conditions. Its overall values for dry core velocities were in the range of 3000-4000 m/s. In addition, low velocity values were associated to high porosity samples. However, several oscillations on the values were noticed and could possibly be related to rock heterogeneities, pore size, different rock composition or other properties that are not macroscopically visible.

When saturated with water the same range of values was registered but, with an increase of velocities when compared to the dry core results. When saturated with brine and hydrocarbons the velocity values slightly increased as well. It was proved that P-waves velocities increase due to a decrease in compressibility thus, saturated core samples present higher velocities in comparison to dry core samples since air is more compressible than fluids. However, it was expected for P-waves velocities in water saturated cores to be higher than in oil saturated core samples since water is less compressible than oil. This, once again, could be related to rock heterogeneities.

Back to hydrocarbons recovery, a more thorough analysis was performed for hydrocarbons elements. When switching the saturation fluid to brine and different hydrocarbons for both porosity and permeability essays, the values increased.

For water and brine the porosity was similar, being the difference between values lower than 1%. For hydrocarbons, porosity was measured for isooctane, n-octane, dodecane and hexadecane. An accentuated difference of porosity values was noticed between water and hydrocarbons, but not between hydrocarbons, due to its lower densities and viscosities. In conclusion, porosity values were similar between hydrocarbons and similar for water and brine.

In this study it was also observed that low porosity samples showed low permeabilities while high porosity samples showed higher permeabilities which indicated that it is expected for this effect to happen regardless of the injection/saturation fluid.

For permeability measurements, isooctane, n-octane, dodecane and hexadecane were also used. When using hydrocarbons with higher molecular weights, it was noticed an increase on the permeability values. However, the difference between values is not relevant ($\pm\ 0{,}022\ \mathrm{mD}$) since they present similar results of permeability, even for brine. Thus, regardless of the saturation fluid, carbonates seem to reproduce similar permeability results.

It was previously discussed that on hydrocarbons fluid flow, there was a preference for lower molecular weight compounds and linear chain alkanes. Since it was noticed an increase in permeability for higher molecular hydrocarbons, then the property that had an influence on the easy percolation of hydrocarbons is likely to be the kinetic diameter. This parameter allowed lower kinetic diameter elements to flow easier when compared to higher kinetic diameter elements, such as isooctane despite the latter's low molecular weight.

Regarding to the binary homogeneous oil mixtures, the permeability values were also similar, which was expected since it was already seen that there was a low variability between hydrocarbons permeabilities. The mixtures selected were isooctane / dodecane and isooctane / n-octane (in different proportions). It was noticed that permeability values increased with higher porosity samples (isooctane / dodecane mixtures), and with higher percentages of lower kinetic diameter components (isooctane / n-octane mixtures).

Even though the mixtures used were homogeneous, its flow was not which means that it was noticed that there was a preferential flow of an element, and it did not occur as a bulk movement. After collecting the effluent from the mixtures permeabilities essays, they were injected on the Gas Chromatograph which indicated the proportion of the mixtures after they percolated the porous media.

For the isooctane / dodecane mixture, two essays with the same proportion and different rock porosities were performed in order to confirm porosity influence on homogeneous oil mixtures. For the lower porosity sample, there was a higher quantity of isooctane (branched alkane and kinetic diameter of 6,2 Å) kept in comparison to the higher porosity one, consequently allowing a higher quantity of dodecane (linear chain alkane and kinetic diameter of 4,6 Å) to flow. With that being said, it is possible for the lower

porosity samples to retain higher kinetic diameter hydrocarbons and branched structure, allowing hydrocarbons with lower kinetic diameter and linear structure to flow through the rock sample.

For the isooctane / n-octane mixture, three essays with different proportions (70/30, 50/50 and 30/70) and similar rock porosities were done. Here, it was observed, for all the core samples, an initial preferential flow of n-octane which also has a linear structure and lower kinetic diameter (4,5 Å) when compared to isooctane.

When comparing this thesis results with the previous work of Hugo Pinto for the disaggregated sandstone rock, it was possible to establish that, sandstones present higher porosity values and consequently higher permeability. Brine, water, and hydrocarbons presented the same behaviour for both rock specimens regarding to porosity but for permeability the opposite happened. On sandstones when increasing the molecular weight, the permeability values decreased. This sample is composed by macro pores hence, the influence of the kinetic diameter was almost irrelevant, allowing the lighter compounds to percolate easier. For binary oil mixtures, sandstones permeability increased with higher percentages of isooctane, reaffirming its preference for lighter compounds. In addition, sandstone samples showed a steadier flow of mixtures, allowing a higher isooctane quantity to flow.

In conclusion, it is possible to say that for rock specimens with a larger pore structure, the kinetic diameter effect is almost negligible. On this type of specimen, lower molecular weight compound has a preferential flow regardless of the kinetic diameter. Thus, kinetic diameter has more influence on carbonate samples (with smaller pores in comparison to sandstones) when compared to sandstones samples.

5.2 Future Work Suggestions

On this thesis some subjects were left in doubt since it was not possible to perform certain experiments to guarantee some of the assumptions, such as the study of carbonate's pore matrix.

For future actions, it would be interesting to analyse the size of pores of carbonate rocks from Codaçal with multiple porosities to understand if a small porosity directly implies small pore sizes. It was previously mentioned that this was a possibility since samples with low porosities kept hydrocarbons with bigger kinetic diameter however, it wasn't confirmed.

Another important aspect that could complement this study is the rock-fluid interactions after the hydrocarbon's mixtures flow, through Thermal Gravimetric analysis. This method will possibly allow the identification of chemical reactions between the rock and the injection fluid.

It will also be interesting to implement different conditions on the core flooding apparatus such as different temperatures, confining pressures, injection fluids (gas or other type of hydrocarbons) and other reservoir rocks.

The comparison between the carbonate rock and the sandstone specimen, from the previous thesis, is only valid for disaggregated sandstones since this was the condition that the rock was handled. It would be interesting to understand if the results from the disaggregated sandstone will remain the same if it was used a consolidated rock instead. Thus, these assumptions made for both rocks could be applied to sandstones in general, regardless of the rock consolidation.

The gathering of these multiple investigations (sandstones and carbonates) along with future works will provide a clearer understanding of fluid flow in reservoir rocks which can enhance future hydrocarbons recovery techniques.

Appendix 1

Table 28 - Perkin-Elmer Claurus 680 Specifications

Gas chromatography (GC) Perkin - Elmer			
Column	BPI	Split	100 mL min^{-1}
Column Length	30m X 250 µm	Injection Temperature	250 °C
Carrier Gas	N_2	Detector Temperature	250 °C
Flow rate	0,5mL min^{-1}	Injection Volume	0,2 µL
Temperature profile: 100 °C for 1 min, 10 °C/ min up to 190 °C, 190 °C for 5 min, 10 °C/ min up to 200 °C and 200°C for 60 min			

Appendix 2

Table 29 - Measurements and P-wave velocity results for dry core samples

Core samples	Core length (mm)	Density (kg/m^3)	Rock Porosity %	Dry core velocity (m/s)
1	90,57	2373,60	10,35	3681,79
2	90,57	2389,91	9,75	3652,18
3	90,47	2299,63	12,92	3301,97
4	90,62	2293,24	13,52	3307,37
5	90,39	2360,66	10,38	3601,35
6	90,47	2301,81	13,19	3119,52
7	90,31	2384,77	10,15	3541,57
8	90,47	2362,72	10,78	3520,08
9	90,53	2395,35	9,34	3725,60
10	90,50	2370,88	10,38	3577,08
11	90,66	2389,35	9,61	3320,73
12	90,29	2311,05	12,62	3356,43
13	90,62	2367,90	10,59	3356,22
14	90,67	2362,55	10,76	3555,84
15	100,22	2343,01	11,69	3796,14
16	101,34	2391,09	10,42	4276,12
17	101,05	2428,94	9,75	4336,74
18	100,85	2341,63	12,31	3970,63
19	99,96	2410,52	9,27	4290,04
20	100,86	2360,92	11,61	4099,84
21	91,70	2308,05	12,56	3836,65
22	91,61	2367,40	10,75	4000,44
23	91,50	2380,27	10,18	4158,86
24	91,21	2391,06	9,70	4364,31
25	91,57	2385,90	9,54	4219,72
26	91,61	2393,49	9,65	3578,52

Table 30 - Measurements and P-wave velocity results for water saturated core samples

Core samples	Core length (mm)	Density (kg/m^3)	Rock Porosity %	Water saturated core velocity (m/s)
1	90,57	2373,60	10,35	4212,65
2	90,57	2389,91	9,75	4193,24
3	90,47	2299,63	12,92	3738,60
4	90,62	2293,24	13,52	3744,71
5	90,39	2360,66	10,38	4184,91
6	90,47	2301,81	13,19	3388,24
7	90,31	2384,77	10,15	4086,43
8	90,47	2362,72	10,78	4002,92
9	90,53	2395,35	9,34	4352,50
10	90,50	2370,88	10,38	3663,97
11	90,66	2389,35	9,61	3640,80
12	90,29	2311,05	12,62	3875,02
13	90,62	2367,90	10,59	3760,08
14	90,67	2362,55	10,76	3793,89
15	100,22	2343,01	11,69	3617,98
16	101,34	2391,09	10,42	4205,15
17	101,05	2428,94	9,75	4263,54
18	100,85	2341,63	12,31	3820,23
19	99,96	2410,52	9,27	4327,19
20	100,86	2360,92	11,61	3909,15
21	91,70	2308,05	12,56	3595,92
22	91,61	2367,40	10,75	3801,24
23	91,50	2380,27	10,18	3960,82
24	91,21	2391,06	9,70	4282,35
25	91,57	2385,90	9,54	4143,35
26	91,61	2393,49	9,65	3343,43

This page intentionally left in blank

References

1- Litvinenko, V. (2020). The Role of Hydrocarbons in the Global Energy Agenda: The Focus on Liquefied Natural Gas. *Resources*, *9*(5), 59

2- Romero-Zerón, L. (Ed.). (2012). *Introduction to enhanced oil recovery (EOR) processes and bioremediation of oil-contaminated sites*. BoD–Books on Demand.

3- Tunio, S. Q., Tunio, A. H., Ghirano, N. A., & El Adawy, Z. M. (2011). Comparison of different enhanced oil recovery techniques for better oil productivity. *International Journal of Applied Science and Technology*, *1*(5).

4- Hamouda, A. A., & Karoussi, O. (2008). Effect of temperature, wettability and relative permeability on oil recovery from oil-wet chalk. *Energies*, *1*(1), 19-34.

5- Satter, A., & M. Iqbal, G. (2016). *Reservoir engineering the fundamentals, simulation, and management of conventional and unconventional recoveries.* Gulf Professional Publishing.

6- Bradley, H B. *Petroleum engineering handbook*. United States

7- Lyons, W. (1996). *Standard Handbook of Petroleum and Natural Gas Engineering (Volume 2).* Butterworth-Heinemann.

8- Salehi, M. M., Safarzadeh, M. A., Sahraei, E., & Nejad, S. A. T. (2014). Comparison of oil removal in surfactant alternating gas with water alternating gas, water flooding and gas flooding in secondary oil recovery process. *Journal of Petroleum Science and Engineering*, *120*, 86-93.

9- Melrose, J. C. (1974). Role of capillary forces in detennining microscopic displacement efficiency for oil recovery by waterflooding. *Journal of Canadian Petroleum Technology*, *13*(04).

10- Willhite, G. P. (1986). Waterflooding.

11- Kamari, A., Nikookar, M., Sahranavard, L., & Mohammadi, A. H. (2014). Efficient screening of enhanced oil recovery methods and predictive economic analysis. *Neural Computing and Applications*, *25*(3-4), 815-824

12- Thomas, S. (2008). Enhanced oil recovery-an overview. *Oil & Gas Science and Technology-Revue de l'IFP*, *63*(1), 9-19.

13- Mokheimer, E., Hamdy, M., Abubakar, Z., Shakeel, M. R., Habib, M. A., & Mahmoud, M. (2019). A comprehensive review of thermal enhanced oil recovery: techniques evaluation. *Journal of Energy Resources Technology*, *141*(3).

14- E. HEINEMANN, Z., & Mittermeir, G. (2014). *PHDG- Natural Fractured Reservoir Engineering.* Tehran.

15- Andersen, M. A., Duncan, B., & McLin, R. (2013). Core truth in formation evaluation. *Oilfield Review*, *25*(2), 16-25.

16- . Mookerjee, A., & Alias, Z. A. (2006, September). Core Analysis Program For A Giant, Complex Fractured Carbonate Field In Oman: Learnings And Key Results. In *SCA2006-19, in Proceedings of the International Symposium of the Society of Core Analysts, Trondheim, Norway* (pp. 12-16)

17- . Ukar, E., Laubach, S. E., & Hooker, J. N. (2019). Outcrops as guides to subsurface natural fractures: Example from the Nikanassin Formation tight-gas sandstone, Grande Cache, Alberta foothills, Canada. *Marine and Petroleum Geology*, *103*, 255-275.

18- Y. Dandekar, A. (2013). *Petroleum Reservoir Rock and Fluid Properties (2nd Edition).* CRC press.

19- E. HEINEMANN, Z., & Mittermeir, G. (2013). *PHDG - Fluid Flow in Porous Media.* Tehran.

20- McPhee, Reed, C., Zubizarreta, J., & Izaskun. (2015). *Core analysis: a best practice guide .* Elsevier

21- Hu, X., Hu, S., Jin, F., & Huang, S. (2017). *Physics of Petroleum Reservoirs.* Springer Berlin Heidelberg.

22- Moore, C. H. (1989). *Carbonate diagenesis and porosity*. Elsevier.

23- Tiab, Donaldson, D., & Erle C. . (2015). *Petrophysics - Theory and Practice of Measuring Reservoir Rock and Fluid Transport Properties.* Gulf professional publishing.

24- *Schlumberger: Global Oilfield Services & Equipment*. (s.d.). Obtido de https://www.slb.com/resource-library

25- Honarpour, M., & Mahmood, S. M. (1988). Relative-permeability measurements: An overview. *Journal of petroleum technology*, *40*(08), 963-966.

26- Honarpour, M. M., Nagarajan, N. R., Orangi, A., Arasteh, F., & Yao, Z. (2012, January). Characterization of critical fluid PVT, rock, and rock-fluid properties-impact on reservoir performance of liquid rich shales. In *SPE Annual Technical Conference and Exhibition*. Society of Petroleum Engineers.

27- Kantzas, A., Bryan, J., & Taheri, S. (2012). *Fundamentals of Fluid Flow in Porous Media.* Pore size distribution.

28- E. HEINEMANN, Z. (2003). *Petroleum Recovery .* Leoben: Montanuniversitat Leoben.

29- Alribi, S. (2016). *The Optimization of Self Assembling Polymeric Systems for Enhanced Oil Recovery.* Doctoral Dissertation, University of New Brunswick.

30- Bacon, M., Simm, R., & Redshaw, T. (2003). *3-D Seismic Interpretation.* United Kingdom: Cambridge University Press.

31- Kahraman, S. (2007). The correlations between the saturated and dry P-wave velocity of rocks. Ultrasonics, 46(4), 341-348.

32- Wang, Z., Hirsche, W.K., and G. Sedgwick. "Seismic Velocities In Carbonate Rocks." J Can Pet Technol 30 (1991): No Pagination Specified. doi: https://doi.org/10.2118/91-02-09

33- Palaz, I., & Marfurt, K. (1997). *Carbonate Seismology.* USA: Society of Exploration Geophysicists.

34- Barton, N. (2007). *ROCK QUALITY, SEISMIC VELOCITY, ATTENUATION AND ANISOTROPY.* London, UK: Taylor & Francis Group.

35- *SMS TSUNAMI WARNING (2018)*. Availabe at https://www.sms-tsunami-warning.com

36- Ahmed, T. (2018). *Reservoir engineering handbook.* Gulf professional publishing.

37- B. Nagy, Review of the chromatographic “plate” theory with reference to fluid flow in rocks and sediments, Geochimica et Cosmochimica Acta 19 (1960): 289 – 296.

38- JONSSON, J. A. 1987. Common concepts of chromatography. In: JONSSON, J. A. (ed.), Chromatographic Theory and Basic Principles. Chromatographic Science Series, 38, Marcel Dekker, New York, 1-25

39- J. A. Curiale, J. B. Curtis, Organic geochemical applications to the exploration for source-rock reservoirs – A review, Journal of Unconventional Oil and Gas Resources 13 (2016):1 – 31.

40- B. M. Krooss, L. Brothers, M. H. Engel, Geochromatography in petroleum migration: a review, Geological Society, London, Special Publications 59 (1991): 149 – 163.

41- MILESHINA A. G., SA.F~NOVA G. I. and KAN~EVA N. A. (1959) The influence of the mineralogical composition of rocks upon oil percolating through them. Geeol. Nefti i Gaza 3, 55-60

42- Leythaeuser D., Bjorgy M., Mackenzie A. S., Schaefer R. G. and Altebaumer F. J. (1983) Recognition of migration and its effect within two coreholes in shale/sandstone sequences from Svalbard, Norway. In Advances in Organic Geochemistry 1981 (Edited Bjorgy M. et al.), pp. 136-146. Wiley, Chichester.

43- J. V. Bonilla, M. H. Engel, Chemical and isotopic redistribution of hydrocarbons during migration: Laboratory simulation experiments, Organic Geochemistry 10 (1986): 181 – 190.

44- A. L. Cheng, W. L. Huang, Selective adsorption of hydrocarbon gases on clays and organic matter, Organic Geochemistry 35 (2004): 413 – 423.

45- B. M. Krooss, D. Leythaeuser, Experimental measurements of the diffusion parameters of light hydrocarbons in water-saturated sedimentary rocks-II. Results and geochemical significance, Organic Geochemistry 12 (1988): 91 – 108.

46- B. M. Krooss, Experimental investigation of the molecular migration of C1-C6 hydrocarbons: Kinetics of hydrocarbon release from source rocks, Organic Geochemistry 13 (1988): 513 – 523.

47- Antonov P. L. (1954) On the diffusion permeability of some claystones. Trudy NIIGGR 2, 39-55. Sb: Geokhim. Met. Poisk. Nefti i Gaza. Gostoptekhizdat, Moscow.

48- Antonov P. L. (I 964) On the extent of diffusive permeability of rocks. Sb: Direct Methods of Oil and Gas Exploration, pp. 5-13. Izd. Nedra, Moscow.

49- Antonov P. L. (1968) Some results of the research on molecular migration of hydrocarbon gases in rocks. Trudy VNIIYaGG 4, 132-154. Izd. Nedra, Moscow.

50- Antonov P. L. (1970) Results of the investigation of diffusion permeability of sedimentary rocks for hydrocarbon gases. Trudy VNI1YaGG 8, 51-79. Moscow.

51- Eyring H. (1936) Viscosity, plasticity, and diffusion as examples of absolute reaction rates. J. Chem. Phys. 4, 283-291.

52- Bradley R. S. (1937) The rate of unimolecular and bimolecular reactions in solution as deduced from a kinetic theory of liquids. Trans. Farad. Soc. 33, 1185-1937.

53- Wheeler T. S. (1938) On the theory of liquids. Trans. Nat. Inst. Sci. India 1, 333-365.

54- Pinto, H. (2020). Universidade de Lisboa, Instituto Superior Técnico. Chemical Transformations in EOR context.
55- Ma, S. M., & Amabeoku, M. (2015). Core analysis with emphasis on carbonate rocks—quality assurance and control for accuracy and representativeness. *Interpretation*, *3*(1), SA91-SA106.
56- Azerêdo, A. C., Inês, N., & Bizarro, P. (2020). Carbonate reservoir outcrop analogues with a glance at pore-scale (Middle Jurassic, Lusitanian Basin, Portugal). *Marine and Petroleum Geology*, *111*, 815-851.
57- Carvalho, J., Manuppella, G., & Moura, A. C. (1998). Contribution to the geological knowledge of the Portuguese Ornamental Limestone. *Comunicações dos Serviços Geológicos de Portugal*, *84*.
58- Carvalho, J. M., Prazeres, C., Lisboa, J. V., & Sardinha, R. (2012). Rochas ornamentais do Maciço Calcário Estremenho: breve caraterização dos recursos, dos centros de produção e delimitação preliminar de áreas potenciais. Boletim de Minas.Carvalho, J. M. F., Manuppella, G., & Moura, A. C. (2003). Portuguese Ornamental Limestones. In *International Symposium on Industrial Minerals and Building Stones, Turkey*.
59- Manuppella G, Antunes A, Almeida CAC, Azerêdo AC, Barbosa B, Cardoso JL, Crispim JA, Duarte LV, Henriques MH, Martins LT, Ramalho MM, Santos V, Terrinha P (2000) Notícia Explicativa da Carta Geológica de Portugal, escala 1:50000, Folha 27-A – Vila Nova de Ourém, 2ª edição, Instituto Geológico Mineiro, Lisboa
60- J. F. Ramos, A. C. Moura, Rochas Ornamentais Portuguesas, Instituto Nacional de Engenharia, Tecnologia e Inovação (2004) Available at: http://rop.lneg.pt/rop/index.php.
61- Hosoya, H. (2002). Chemical meaning of octane number analyzed by topological indices. *Croatica chemica acta*, *75*(2), 433-445.J. H. Al-Fahemi, N. A. Albis, E. A. M. Gad, QSPR models for octane number prediction, Journal of Theoretical Chemistry (2014):1 – 6.
62- Seng-eiad, S., & Jitkarnka, S. (2015). Estimation of Average Kinetic and Maximum Diameters of Hydrocarbon Groups in Tyre-Derived Oil for Catalyst Design Purpose. Chemical Engineering Transactions, 45, 895-900.
63- R. H. Perry, D. W. Green, J. O. Maloney, Perry`s Chemical Engineer`s Handbook, Seventh Edition, McGraw-Hill, 1997.
64- Grabski, E. (2012). *Matrix Acidizing Core Flooding Apparatus: Equipment and Procedure Description* (Doctoral dissertation).
65- A. Baldygin, D. S. Nobes, S. K Mitra, A new laboratory core flooding experimental system, Industrial & Engineering Chemistry Research (2014): 1 – 26.
66- McNair, H. M., Miller, J. M., & Snow, N. H. (2019). *Basic gas chromatography*. John Wiley & Sons.
67- Bartle, K. D., & Myers, P. (2002). History of gas chromatography. *TrAC Trends in Analytical Chemistry*, *21*(9-10), 547-557.
68- Gabbott, P. (Ed.). (2008). *Principles and applications of thermal analysis*. John Wiley & Sons.
69- Ahr, W. M. (2011). Geology of carbonate reservoirs: the identification, description and characterization of hydrocarbon reservoirs in carbonate rocks. John Wiley & Sons.

70- C. Figueiredo, R. Folha, A. Maurício, C. Alves, L. A. Barros, Contribution to the technological characterization of two widely used Portuguese dimension stones: the 'Semi-rijo' and 'Moca Creme' stones, Geological Society, London, Special Publications 333 (2010): 153 – 163.

71- C. Alves, C. Figueiredo, A. Maurício, M. A. S. Braga, L. A. Barros, Limestones under salt decay tests: assessment of pore network-dependent durability predictors, Environmental Earth Sciences Journal 63 (2011): 1511 – 1527

72- Ghabezloo, S., Sulem, J., Guédon, S., & Martineau, F. (2009). Effective stress law for the permeability of a limestone. International Journal of Rock Mechanics and Mining Sciences, 46(2), 297-306.

73- Kahraman, S., & Yeken, T. (2008). Determination of physical properties of carbonate rocks from P-wave velocity. Bulletin of Engineering Geology and the Environment, 67(2), 277-281.

74- A.R. Gregory, Fluid saturation effects on dynamic elastic properties of sedimentary rocks, Geophysics 41 (1976) 721–895.

75- M.R.J. Wyllie, A.R. Gregory, L.W. Gardner, Elastic wave velocities in heterogeneous and porous media, Geophysics 21 (1956) 41–70.

76- R.D. Lama, V.S. VutukuriHandbook on Mechanical Properties of Rocks, Vol. 2, Trans Tech Publications, Clausthal, Germany, 1978.

77- Oliveira, G., Ceia, M., Missagia, R., Santos, V., & Neto, I. L. (2016). Permeability dependence of porosity and p-wave velocity in carbonate rocks. In SEG Technical Program Expanded Abstracts 2016 (pp. 3272-3276). Society of Exploration Geophysicists.

78- National Center for Biotechnology Information (2021). PubChem Compound Summary for CID 8182, Dodecane. Retrieved August 16, 2021 from https://pubchem.ncbi.nlm.nih.gov/compound/Dodecane.

79- Jiménez-Cruz, F., & Laredo, G. C. (2004). Molecular size evaluation of linear and branched paraffins from the gasoline pool by DFT quantum chemical calculations. Fuel, 83(16), 2183-2188

80- A. K. Aboul-Gheit, S. M. Ahmed, S. A. Hanafy, Exchanged zeolites with transition metals of the first period as photocatalyts for n-hexadecane degradation, Journal of Molecular Catalysis A: Chemical 288 (2008): 52 – 57.